

# Mechanical Report

---

University of British Columbia

Solar Car Team

# Outline

## Table of Contents

Contact Information.....	3
Introduction .....	3
Vehicle Overview .....	3
<b>Mechanical System Analysis .....</b>	<b>4</b>
Front Suspension.....	4
Rear Suspension .....	7
Brakes .....	10
Steering .....	14
Wheels and Tires .....	16
Battery Enclosure.....	17
Seat Belts.....	21
<b>Vehicle Impact Analysis .....</b>	<b>23</b>
Specifications.....	23
Drawings .....	24
Analysis .....	26
Conclusions .....	36
<b>Appendix</b>	
Appendix A (Mechanical Systems Analysis).....	37
Appendix B (Vehicle Impact Analysis) .....	46

# Introduction

## Contact Information

*Mechanical Lead (Primary Contact)*

Svena Yu

+1 778 706 5535, svena.yu@ubcsolar.com

*Captain*

David Schwartz

+1 604 313 5837, manager@ubcsolar.com

## Introduction

The Solar Car Team at the University of British Columbia comprises of a group of undergraduate students from diverse backgrounds, from first year students to engineering physics. The team was started in the later half of year 2009, by several students passionate about combining racing and solar power. With the help of many other engineering students, faculty and machinists, we now present our first full design and fabrication cycle. Being our first car, we have decided on a standard three-wheeled configuration, with a large composite shell and a spaceframe.

## Vehicle Overview

*Raven* is the solar vehicle designed and built by UBC Solar. The vehicle has two wheels on the front and a wheel on the back. The structural spaceframe, which is our rollcage, is primarily constructed out of AISI 4130 chromoly steel, TIG welded together. The rollcage forms the primary structural and driver safety components, with the aeroshell provides the main aerodynamic properties of the car.

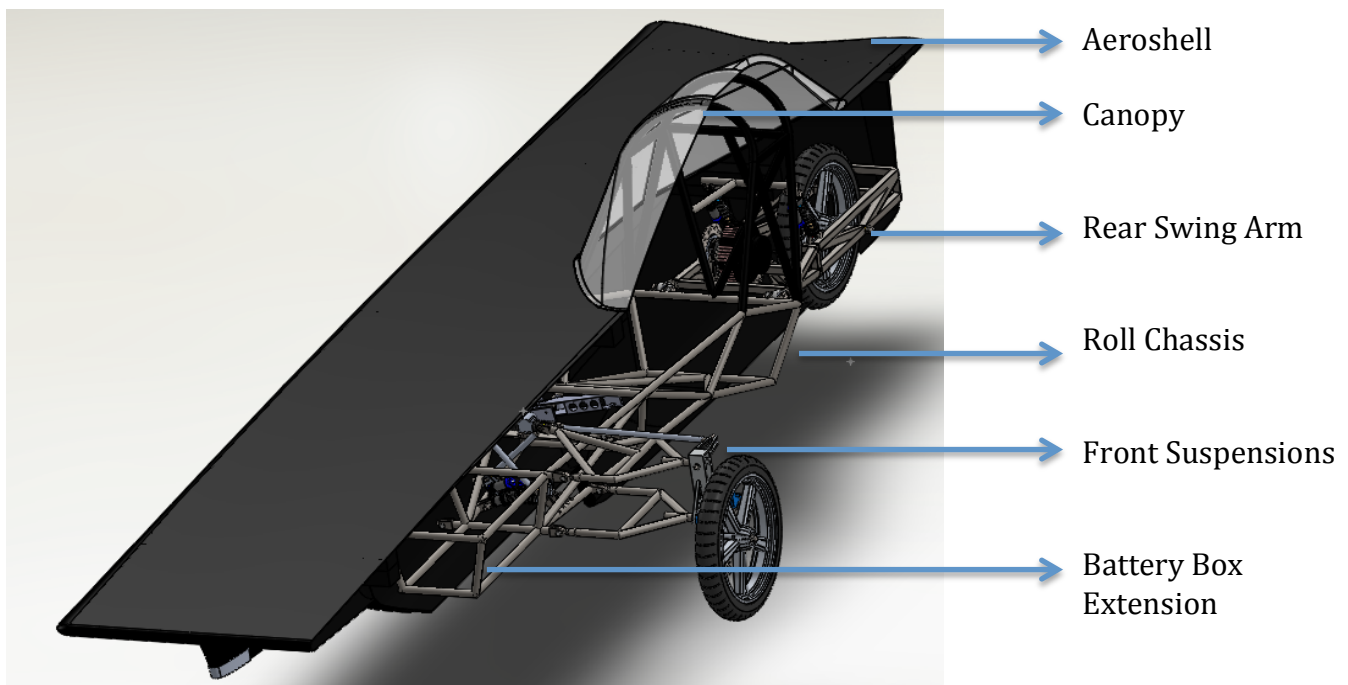


Figure 1. Cutaway view of fully assembled car

# Mechanical System Analysis

## Front Suspension

### Overview

The front suspension is a double wishbone assembly with a push rod suspension. The two control a-arms are connected to the upright with rod-end bearings, which in turn houses the brake callipers and the front axle. The choice to design a push rod assembly that is housed within the rollcage is due to preliminary calculations and testing, which showed that the suspension system, if external, will increase drag by nearly 30%.

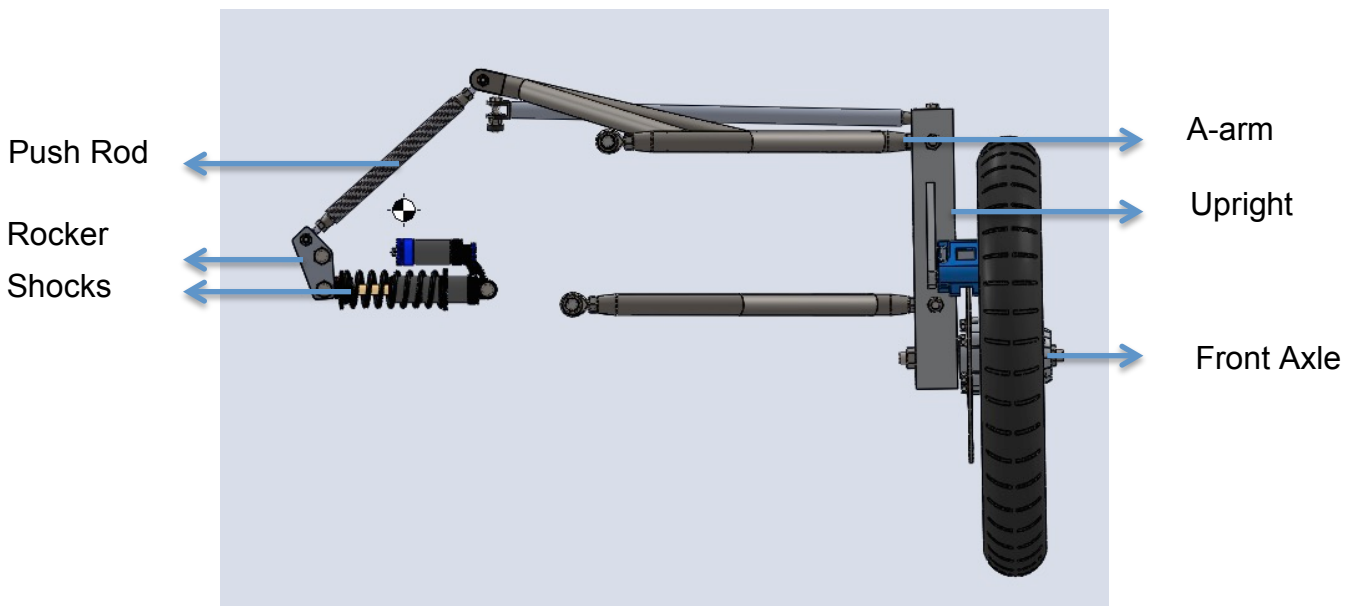


Figure 2. Front Suspension Assembly (Side View)

### Material Specifications

The front suspension consists of an upper A-arm, a lower A-arm, an upright, a shock, a rocker and a push rod.

Part	Material/Details	Construction
Upper A-arm	4130 Chromoly Steel	Cut, notched and welded at the joints
Lower A-arm	4130 Chromoly Steel	Cut and welded together
Push Rod	Aluminium 6061-T6	CNC-milled
Rocker	Aluminium 6061-T6	Waterjet, welded then heat treated
Upright	Zinc Plated Steel	From McMaster Carr
Bolts	Heat treated Alloy Steel	Aurora Bearings AM-5, AM-7

Shocks	-	Fox DHX 5.0 Shocks
--------	---	--------------------

### ✿ Control Arms

The two a-arms of unequal length are made from 1" OD x 0.065" wall thickness 4130 chromoly steel round tubing. They are notched and welded to tapped tube end weld nuts, which is where the 7/16"-20 UNF rod end bearings are attached to.

The rod end bearings made of high strength, heat treated alloy steel from Aurora. They are connected to the main frame by 7/16"-20 UNF bolts.

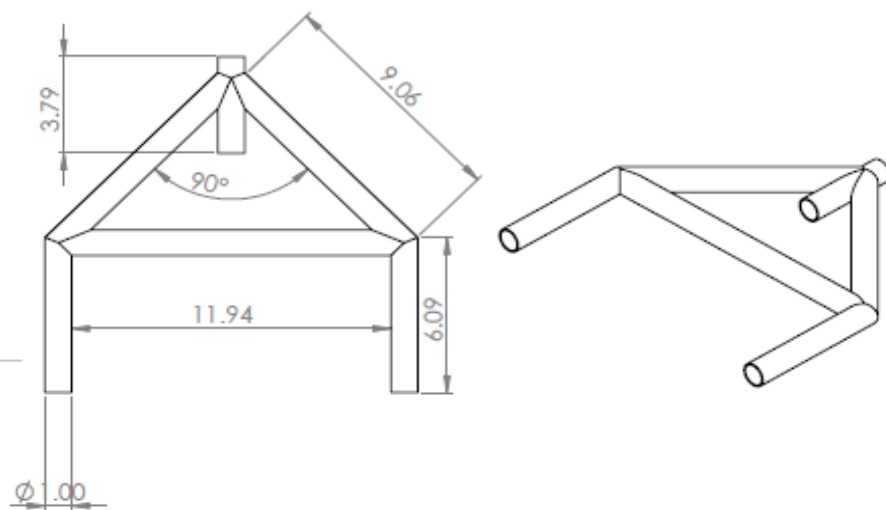


Figure 3. A-arm Dimensions

### ✿ Push Rod

There are two push rods connected to aluminium rockers. Each push rod is made of  $\frac{3}{4}$ " OD x 0.065" wall thickness 4130 chromoly steel round tubing. Each end is welded to tapped tube end weld nuts with 5/16"-24 UNF rod-end bearings.

### ✿ Rocker

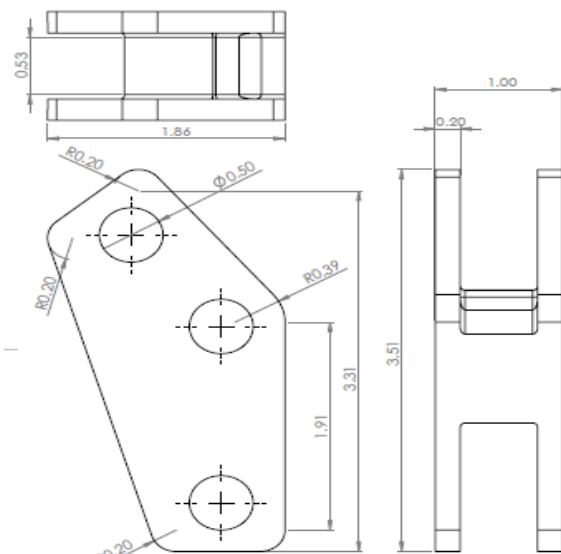


Figure 4. Rocker Dimensions

The rocker is a component that transmits pushrod motion into the shock absorber through a lever mechanism. It is CNC machined out of 6061-T6 aluminum, and it has three holes for bolts to mount onto.

## ⚙️ Upright Assembly

The upright assembly consists of two brackets for the brake callipers and two steering rod mounts. The cross-sectional dimensions of the tube used is a two inch square with a thickness of  $\frac{1}{4}$  inches. The calliper brackets are welded and then heat treated in an oven at 400°F for 90 minutes. This process relieves residual stresses and restores most of the aluminium's strength after the intense heat experienced during welding.

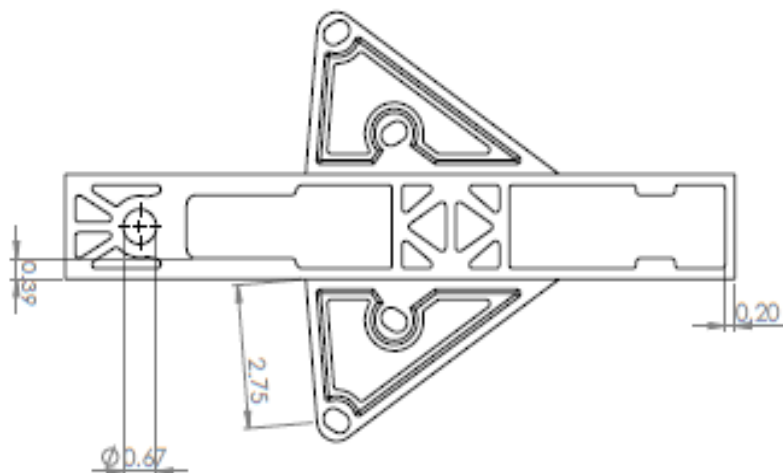


Figure 5. Upright Dimensions

## ⚙️ Suspension Shocks

The shocks are designed and manufactured by Fox Racing, for the intended purpose of downhill mountain biking. They are Fox DHX 5.0 Shocks, with the dimensions 7.5"x2.0" and the springs used has a spring rate of 500lb/in with 2.8" travels. As mountain biking has similar forces (250lbs over two wheels for mountain biking versus 600lbs over three wheels for the solar car, with mountain biking impacts being much harder), these shocks should be more than sufficient in strength.

## Loading Conditions

---

Impact on the front suspension occur from the loads on the wheel being transmitted to the chassis through the uprights. Major assumptions are that the chassis is rigid. I.e. in the FEA models, the translation of the connection point between a component and the chassis is constrained in all three coordinate directions. A rigid chassis will put more loading on the front suspension system, and is therefore a valid assumption.

We assume the rod end bearings to be perfectly rotating and that the wheel, upright and arms of the chassis are perfectly rigid structures that transmit all loadings without any damping.

# Rear Suspension

## Overview

The rear suspension is a swing arm assembly that houses the drivetrain of the car, which includes the motor, drivetrain and the wheel of the car. The trailing swing arm is attached to the main chassis via shock absorbers and rod-end bearings. The rod-end bearings will be bolted to  $\frac{1}{4}$ " chromoly tabs welded to the rollcage.

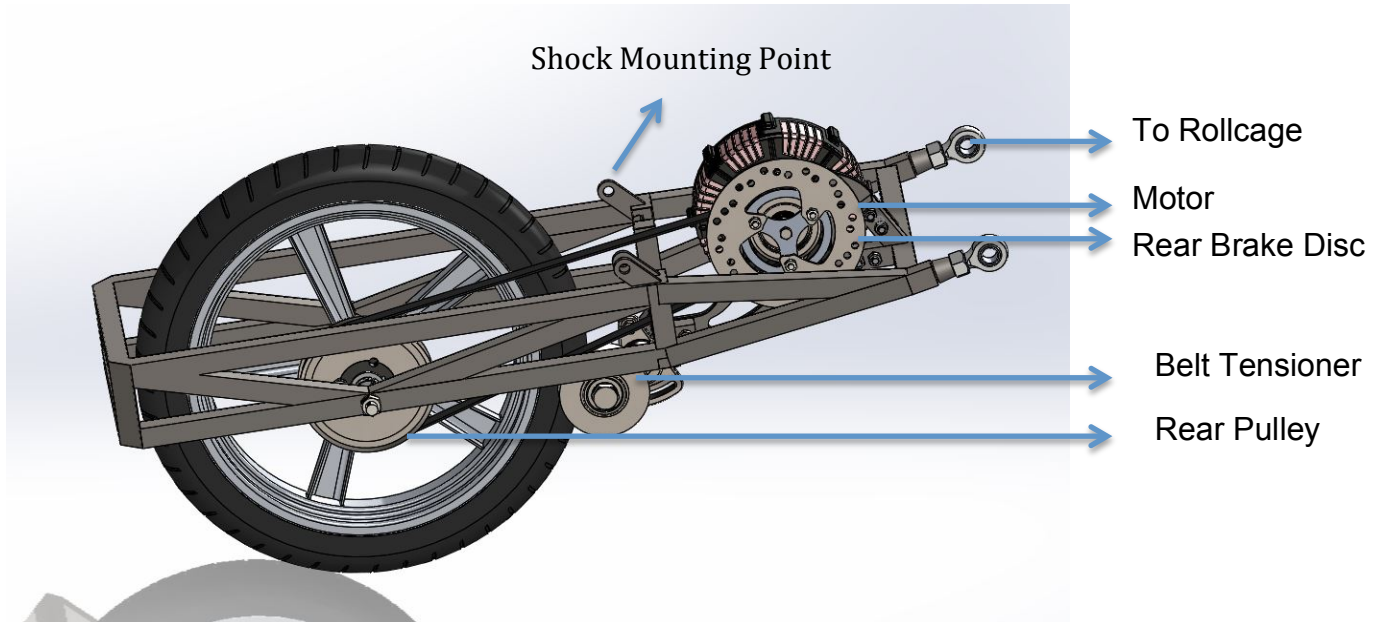


Figure 6. Rear Swing Arm Assembly

## Material Specifications

The rear suspension consists of a swing arm, two  $\frac{1}{2}$ " rod ends, and two Fox DHX shocks. The swing arm is a chromoly truss structure, designed to engage the shocks but minimize torsion and bending within the swing arm.

Part	Material/Details	Construction
Swing Arm Frame	4130 Chromoly Steel	Cut, notched and welded at the joints
Bolts	Zinc Plated Steel	From McMaster Carr
Rod-End Bearings	Heat treated Alloy Steel	Aurora Bearings AM-12
Rear Axle	Cold Rolled Ground Steel Shaft	Cut grooves on lathe
Shocks	-	Fox DHX RC4
Front Pulley	Gray Iron	Gates P144-8MGT-30
Rear Pulley	Gray Iron	Gates P24-8MGT-30
Timing Belt	Carbon Fibre	PolyGrip GT2

The single rear drive wheel is surrounded by the swing arm on its sides and is connected by a 15mm diameter carbon steel shaft which we machined. The wheel sits on two steel bearings in the wheel hub. On the physical swing arm, the axle is attached using two FS P205 pillow bushing, rather than being run through the chromoly bars themselves. The axle is tapped on both ends and will be secured with nuts at both ends. The axle nuts, rod end bearings and the suspension shocks will be safety wired as they are identified to be critical fasteners.

### ❖ Swing Arm Frame

The rear swing arm frame is made out of square 1"x1" chromoly tubing with a wall thickness of 0.03", notched and tig welded together.

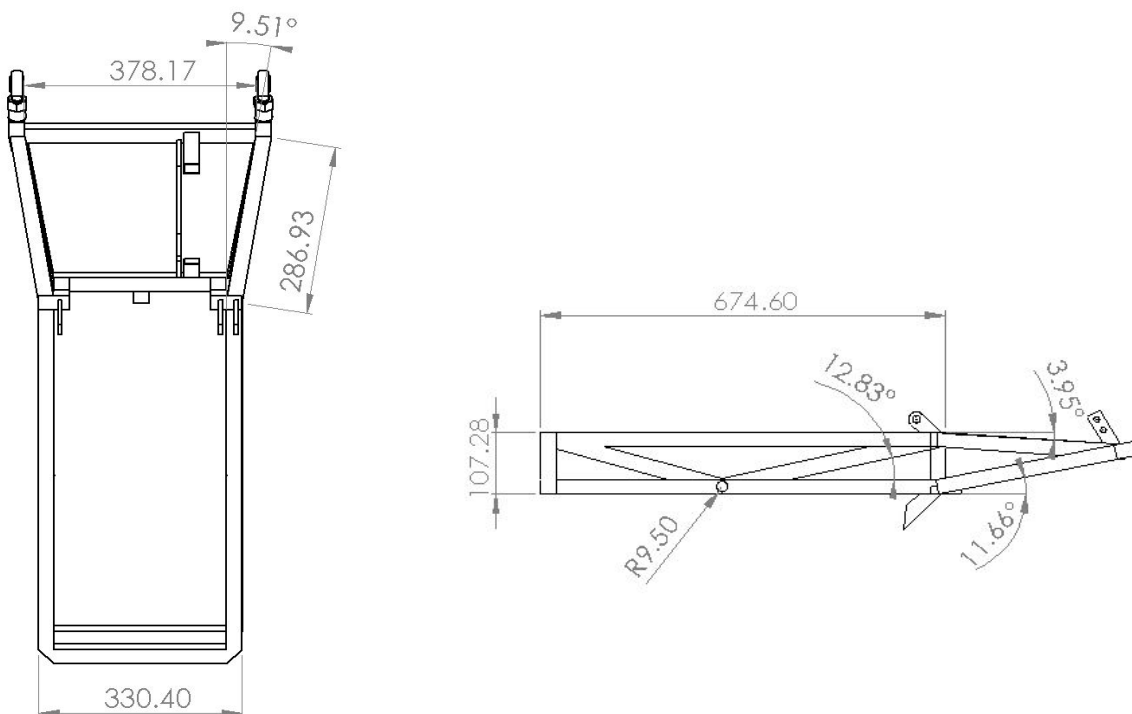


**Figure 7. Rear Trailing Arm Frame w/ Dimensions**

### ❖ Rear Axle Assembly

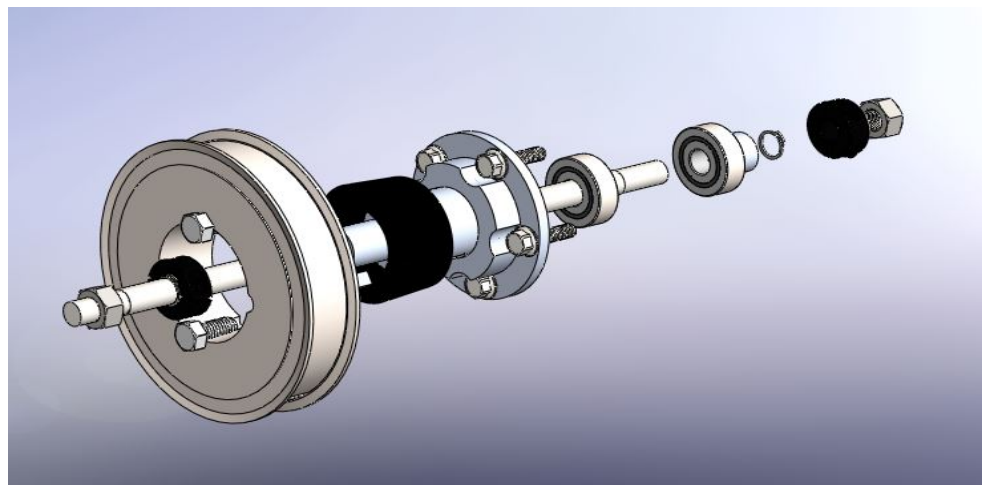


**Figure 8. Rear Axle Components- Exploded view**

## Loading Conditions

The rear suspension is analyzed for a 2G bump, a 1G turn, and a 1G braking load. For all loading conditions, finite element analysis was performed on each component individually working through the system piece by piece. All components besides the one being tested were considered to be fixed and solid, placing the full stress on the single component. We used line elements in ANSYS as a good approximation to analyse the rear swing arm frame.

### a.1G Braking

For braking, the entire weight of the car is applied as the loading vector and is assumed to act backwards at the center of the wheel. In addition, there is a torque in the direction of the axle's rotation that has the potential to shear the bolts in the wheel adapter.

A force of 2580N was applied backwards (in the x direction) on the rear wheel bearings with the ends of the axle being held as fixed supports.

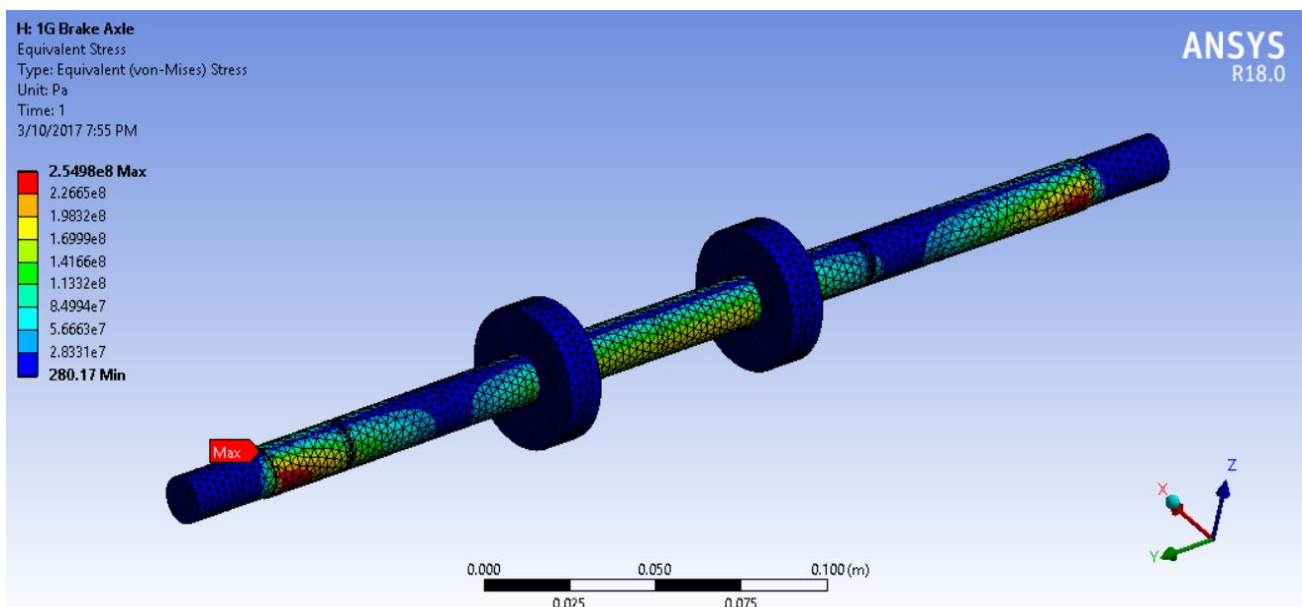


Figure 9. Von-mises Stress Distribution Profile on Rear Axle

Maximum Stress	Yield Stress	Factor of Safety
250MPa	625MPa	2.5

### b.1G Cornering

The entire weight of the car is assumed to be applied as a force perpendicular to the wheel at the point of contact with the road. This causes both a force parallel to the axle, as well as a torque along the length of the axle. No extensive simulations was done as this is not a critical point of failure.

## c.2G Bump

The load is considered to act vertically upwards at the contact point of the tire with the road. The magnitude of this force is twice the weight on the rear wheel. The weight on each wheel was calculated based on the center of mass obtained from the SolidWorks model, and was determined to be 240lbf. Doubling this gives the 480lbf (2135N) used in the finite element analysis.

A force of 2135N was applied upwards on the frame where the axle mounts. The red arrows in the picture show where the force was applied and the red edge is a fixed support.

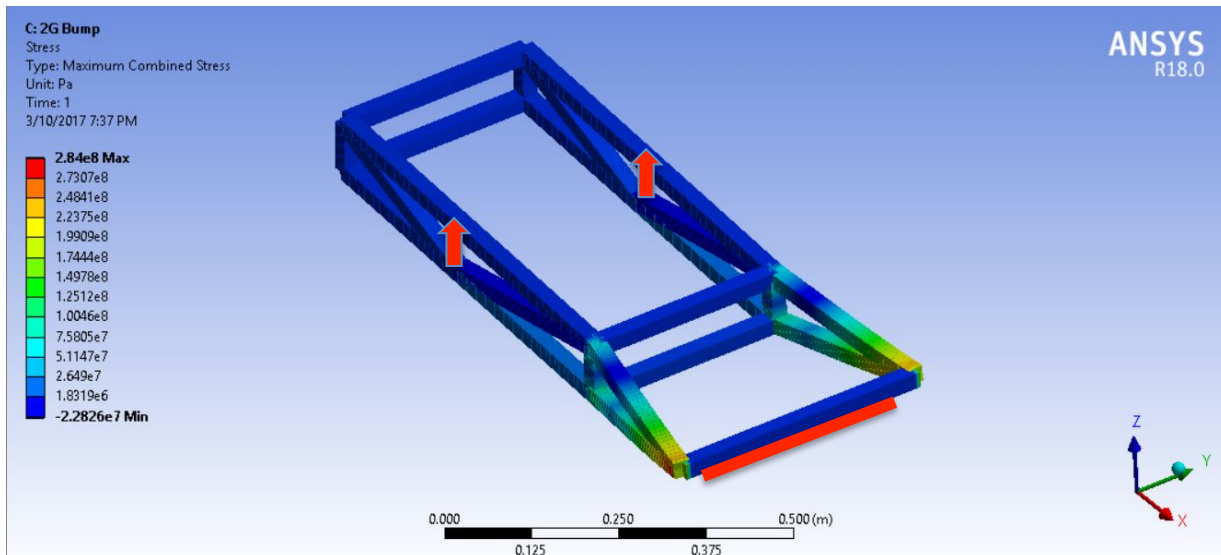


Figure 10. Ansys Simulation of Rear Swing Arm Frame

Maximum Stress	Yield Stress	Factor of Safety
284MPa	568MPa	2.0

## Brakes

### Overview

The main braking system will be the regenerative system built into the powertrain. We have a redundant front braking system which will include two brake callipers on each wheel and a parking brake system. The parking brake system will only be used to counteract static loading on the car and hence will not be formally analysed in this section.

### Material Specifications

The braking system consists of four calipers, two on each brake rotor, the brake pedal and the pedal mount which allows the brake pedal to have three lateral positions. There are brake lines running from the brake pedal to the calipers which carry DOT 4 braking fluid.

Part	Material/Details	Construction
Calliper with Brake Pads	Cast Aluminium	Westwood Billet Go-Kart 120-5750
Bolts (Brake Pedal)	Zinc yellow-chromate plated steel screws	Mcmaster Carr Grade 8 Bolts
Bolts (Brake Rotor to Wheel)	-	Aprillia M8X30 JCA20178030JN00
Brake Rotor	1986 Suzuki GSXR GSX-R750 Motorcycle	Aprilia JC59211X92000
Brake Lines	Stainless steel braided hoses	JEGS 63010148ERL
Brake Pedal	Dual Master Cylinder Brake Pedal Assembly	CNC 204SD
Brake Pedal Mount	Chromoly Steel Plate	Waterjet and welded to the frame

The bolts connecting the brake rotor to the wheel is a flanged hex bolt which is manufactured by Aprilia to match the brake rotor and the wheel hub, both of which are also manufactured by Aprilia.

### Brake Line Layout

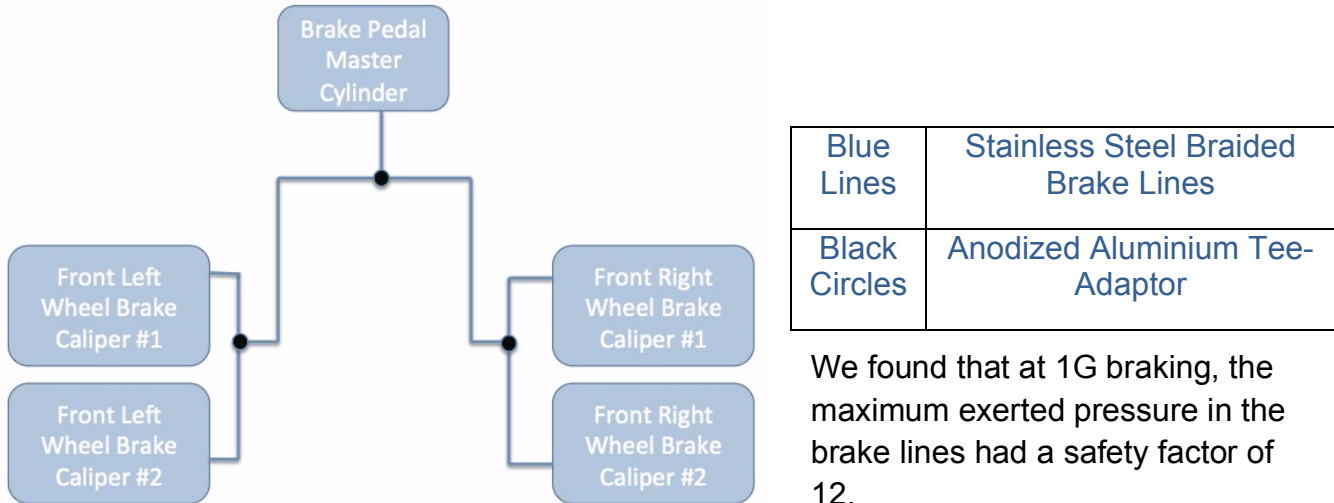


Figure 11. Brake Line Layout

### Brake Calliper

The brake callipers are mounted to the upright assembly and each have one piston of area  $0.79\text{in}^2$ .

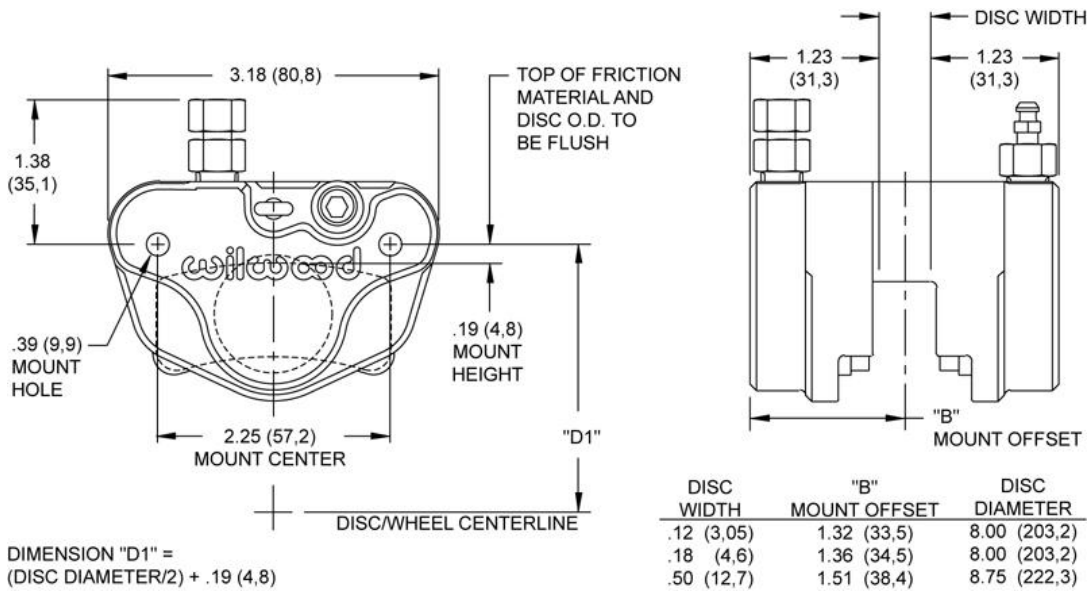


Figure 12. Drawing of Westwood Brake Calliper

### ⚙️ Brake Pads

The brake pads have an area of 15.5cm<sup>2</sup>, and are made out of sintered metal which has a high coefficient of friction (0.6 at 200°F) and resists wear and tear.

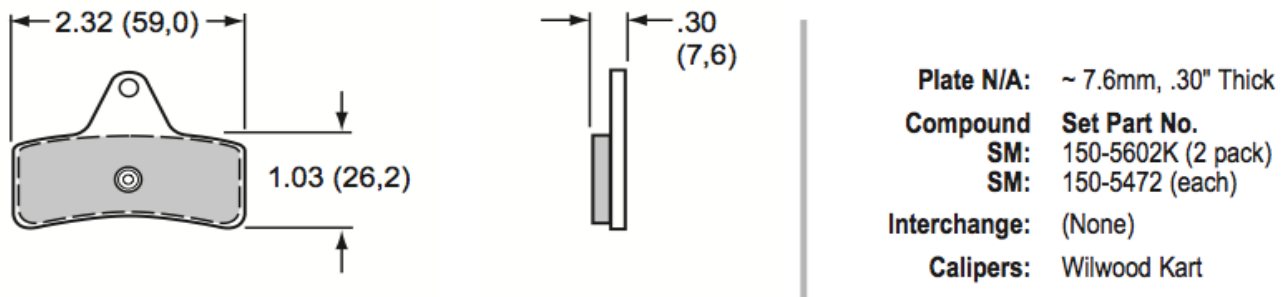


Figure 13 Brake Pads Drawings

### ⚙️ Brake Pad Life

On a regular car brake pads typically last 50 000 to 115 000 kilometers. Thus, even if we doubled this distance we would still be under half of the life expectancy of the brake pads so we expect one set of brake pads will be able to perform throughout the entire race.

### ⚙️ Disk Warpage

Our brake pads have a max operating temperature of 482°C (900°F). If the pads reach this temperature they can cause permanent damage to the braking systems, such as varying rotor thickness which causes shaking in the steering when braking.

We estimate our car will not see speeds much over 80 km/hr so we will use that speed as a max value. Assuming the brake pads start at 30 °C, and 100% of the heat from braking will

be transferred to the brake pads (which is a very conservative assumption), we found that we are well within the manufacturer's the maximum operating temperature as the maximum temperature that the brake pads will reach is 138°C. The disc brakes will also reach a maximum temperature of 75°C, which is much smaller than the maximum specified temperature.

### ● Brake Rotor

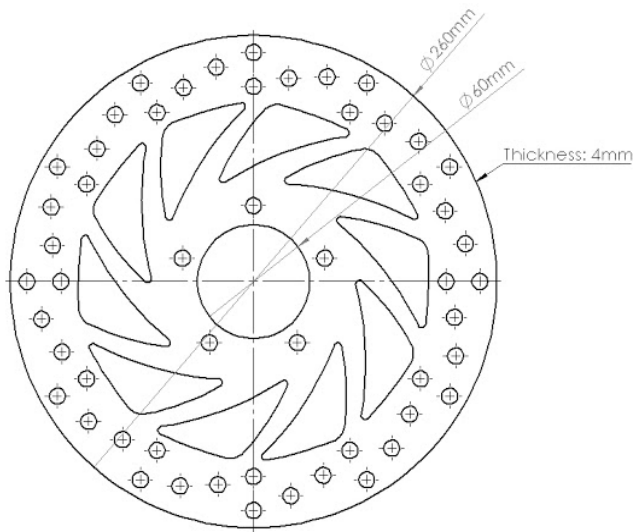


Figure 14. Suzuki Brake Rotor

### ● Brake Pedal

The brake pedal is a master dual cylinder steel brake pedal of the following dimensions and is rated for either DOT 3 or DOT 4 automotive brake fluid.

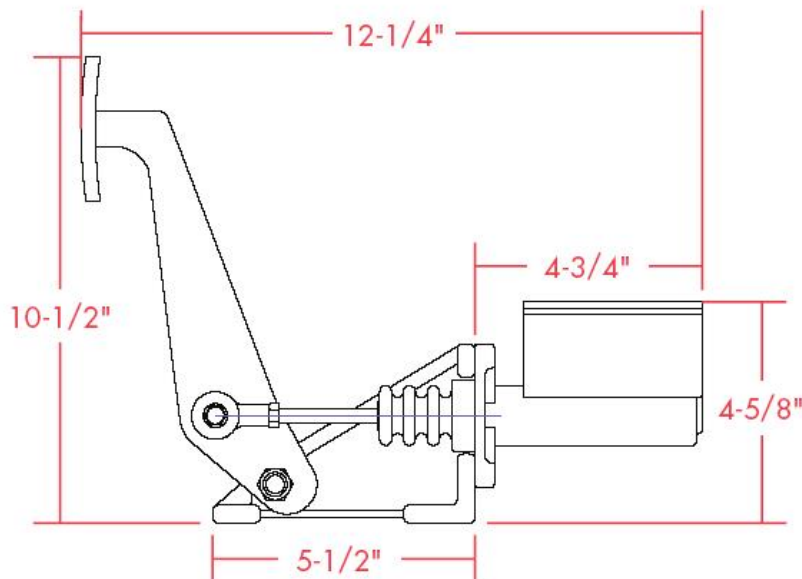


Figure 15. Dimensions of Brake Pedal Assembly

## Loading Conditions

---

The main loading condition in the three scenarios of a 1G turn, a 2G bump, and 1G braking case that is essential for evaluating our braking system is the 1G braking loading scenario.

To calculate the braking force, we assume that there is negligible hydraulic pressure drop during the translation of applied pedal force to caliper force exerted. This is a fair assumption as each of our brake lines only has two 90 degree connector and all four brake lines going to the front two wheels sum up to around 6 ft in total.

### a.1G Brake

For our car of around 341 kg with the driver and ballast, 1G braking force is equivalent to 3345N. For a force of 3345N to be applied by the calipers onto the wheel rotors, the driver has to input a force of **405N**.

Considering that the upper limit of force that the driver is able to exert normally is around 500N of force, we can safely assume that the driver can exert this amount of force with ease.

## Steering

### Overview

---

The steering assembly consists of a rack and pinion, two tie rods, two rod ends, and a connector to the uprights. It is a simple steering system with one linkage at the uprights. The steering ratio is 12:1, which is at the lower end of the spectrum but is suitable for racing purposes. The steering stops will be mounted accordingly on the steering rack mount to limit the steering to less than 15° of turning (hence, 30° in total).

The circles below mark where the rod end connections are.

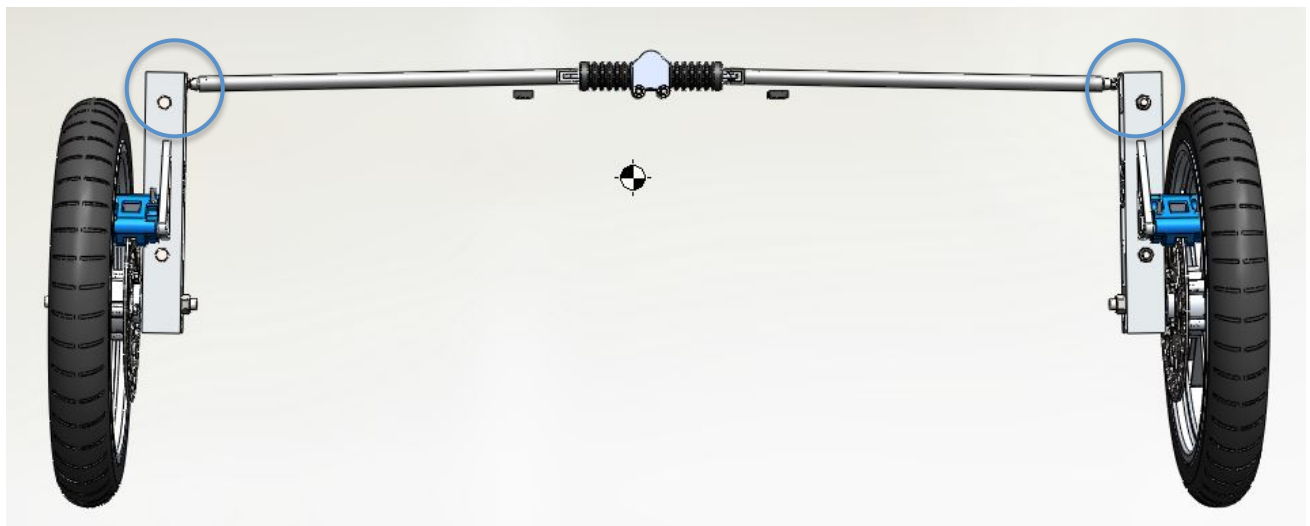


Figure 14. Isolated steering system

## Material Specifications

Part	Material/Details	Construction
Rack and Pinion	Stiletto rack & pinion, High strength steel and aluminium	ProWerks CM-6, 3/8" rod ends
Tie Rod	4130 Chromoly Steel	Machined, welded
Steering Rod Mount	Aluminium 6061-T6	CNC-milled
Rod End Bearings	High strength steel	Aurora Bearings AM-5
Steering Stops	Neoprene Rubber, Steel Base Plate	Mcmaster Carr, 9306K14
Steering Rack Mount	1/8" Mild Steel Sheet	Waterjetted, Bent, Welded

The rack and pinion is manufactured by ProWerks, with the part number C42-340. The tie rods are chromoly with a  $\frac{3}{4}$ " outer diameter with an 0.065" wall diameter. They are welded to tube end weld nuts which are also made of 4130 chromoly steel.

The steering rack mount is a box with rounded side edges, made by bending a 1/8" steel sheet and then welded at bends for structural rigidity. Plates were further welded on the steering rack as attachment points for the rack and pinion. Calculations can be provided upon request as we have not considered the steering rack mount to be a major point of failure.

### • Rack and Pinion

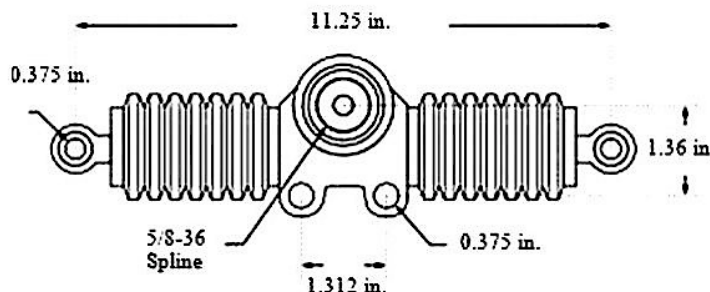


Figure 16. Dimensions of Rack and Pinion from ProWerks

## Loading Conditions

Analysis was carried out to test the system under 1g cornering, 1g braking, and 2g bump. The tie rods would be under near linear tension-compression forces in the 1G cornering scenario. However, in a realistic situation the steering system would experience much smaller loads since most of the forces will be absorbed by the front suspension.

Because of this no extensive analysis will be done on the steering system. The rack and pinion is manufactured for use in drag racing thus it is designed to take loads much greater

than those experienced in our car. The steering column is analyzed when a 70Nm torque is applied by the driver and was found to have a safety factor of close to 6.5. As the steering column will not be subject to much higher loads than the torque calculated, the safety factor we have found is more than adequate for our purposes.

## Wheels and Tires

### Overview

Our car uses Aprilia E 16x2.6 DOT-D wheels mounted to Cheng Shin Tires CST 100/80-16 tires. Both have passed US DOT regulations for highway use, so are appropriate for solar car highway use. The axle of every wheel sits on two wheel bearings each.



**Figure 16. Assembly of the wheel and tire, with the tread visible**

We chose to use motorcycle tires as they are lighter and narrower than conventional automotive tires, which will help reduce our unsprung weight and aerodynamic drag. The manufacturer guarantees cornering and braking under both wet and dry conditions due to the relatively deep shoulder tread of the wheel.

### Material Specifications

Part	Material/Details	Construction
Wheel	Cast Aluminium	Aprilia JC54110X92000
Tire	Nylon Rubber	Cheng Shin Tires CST 100/80-16
Wheel Bearings	52100 Steel	Mcmaster Carr 5972K83 (FAG)

The Aprilia E 16x2.6 DOT-D wheels have a outer diameter of 43.5cm and a width of 8.1cm. The Cheng Shin Tires CST 100/80-16 tires have a inner diameter of 43.7cm, a width of 9.3 cm and the thickness is 6 cm. When the tires are mounted on the wheel, the fully assembled wheel is 55cm in diameter and 10cm in width.

We are using sets of 15mm ID, 42mm OD double sealed steel wheel bearing from FAG. The axles that are supported by the wheel bearings are ground carbon steel shafts that are precisely machined with very low tolerances to reduce wear and tear on the bearings casings.

### ⚙️ Wheel

The approximate tire contact patch is  $40\text{cm}^2$  and the tire is rated for 250kPa maximum pressure. The pressure at the tire contact patch is 26.25kPa at the front and 35.5kPa at the back.

### ⚙️ Wheel Bearing

The maximum radial static loading is rated for 549kg.

Bearing Position	Rated for Weight	Factor of Safety
Front / Rear Wheel	353kg	3.11

We will also not exceed the maximum speed for the bearings. At 18,000rpm, the car will be travelling at approximately 25km per minute, which is an impractical amount and we will certainly be well under that number.

## Battery Enclosure

### Overview

---

The battery enclosure (Figure 1) houses four battery cells, the battery management system, 12V DC-DC converter, two 80mm fans, electrical system fuse, and the system contactor.

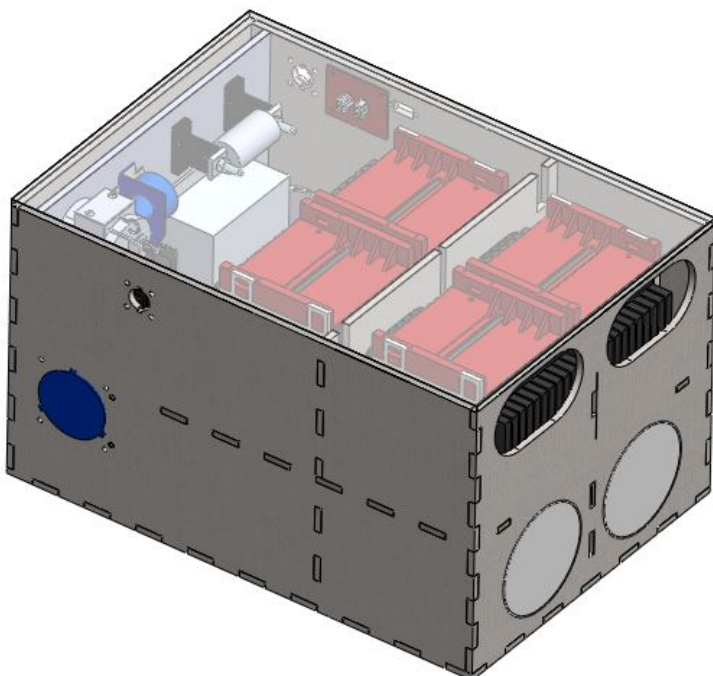


Figure 17. Battery Enclosure Model

## Material Specifications

---

The walls of the enclosure are constructed from composite sandwich panels and the lid is made of a  $\frac{1}{4}$ " polycarbonate sheet. The sandwich panels are constructed commercially by bonding 8oz. 8-harness satin weave fiberglass prepreg to each side of a  $\frac{1}{8}$ " 3PCF aramid honeycomb core. There are 2 plies of fiberglass fully consolidated and bonded to each side of the core cell. This results in a very high strength to weight ratio, which is ideal for our use.

Part	Material/Details	Construction
Battery Enclosure	2 ply 8oz. satin weave fiberglass on each side bonded to $\frac{1}{8}$ " cell, 3 PCF aramid honeycomb core.	Waterjet Cut & Bonded with Epoxy H8000
Battery Enclosure Lid	$\frac{1}{4}$ " Clear Polycarbonate Sheet	Waterjet
Battery Attachment	U bolts and angle irons	Manufactured by retailer
Structural Components in Box	ABS	3D Printed

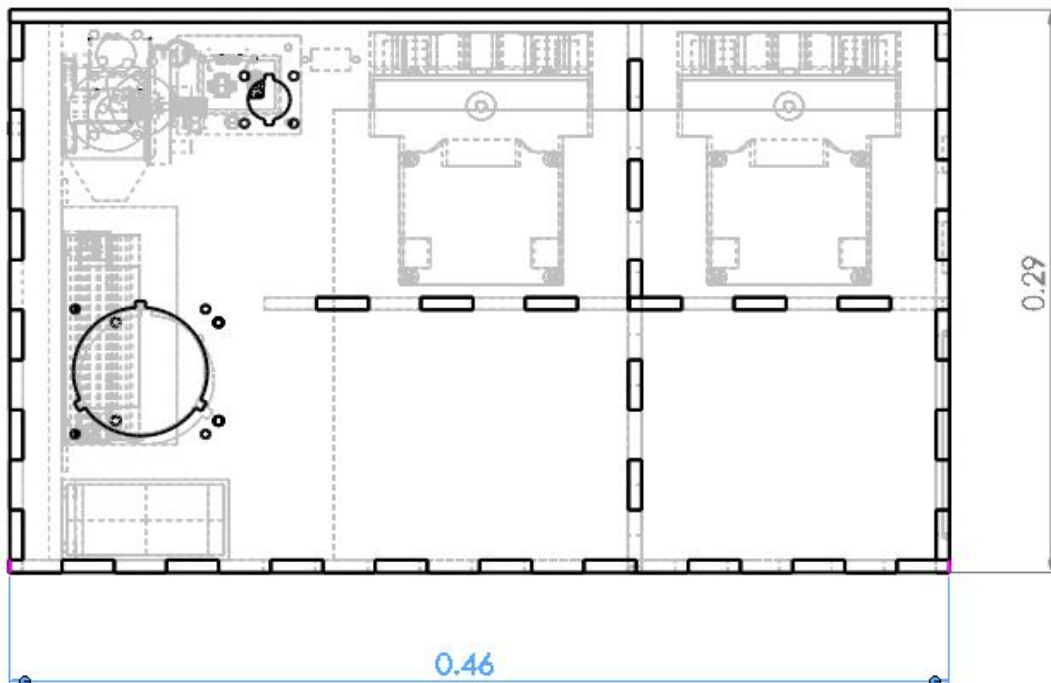


Figure 18. Dimensions of Battery Box Enclosure

The enclosure is attached to the rollcage by an angle iron that connects to a U bolt. The main constraints will be the geometry of the rollcage itself and the main function of this attachment is to minimize movement of the battery box in the longitudinal direction in the scenario of a frontal impact.

Attachment of the battery cell modules to the enclosure is by constraining them in a fitted hole in the fibreglass panels as shown above. The modules are hence held in place by the

fibreglass panels and the geometry of the battery box. The battery caps were extended in height to provide a clamping force on the battery modules and to reduce vertical movement during driving. The electronics will be mounted on a fibreglass sandwich panel in the battery box, which will be physically spaced off from the exterior wall. We will be bolting metal bolts into the box directly and applying varnish on the threaded end of the bolt that is inside the box. This will not affect the electrical isolation as the design has eliminated contact between electrical components and the metal bolts.

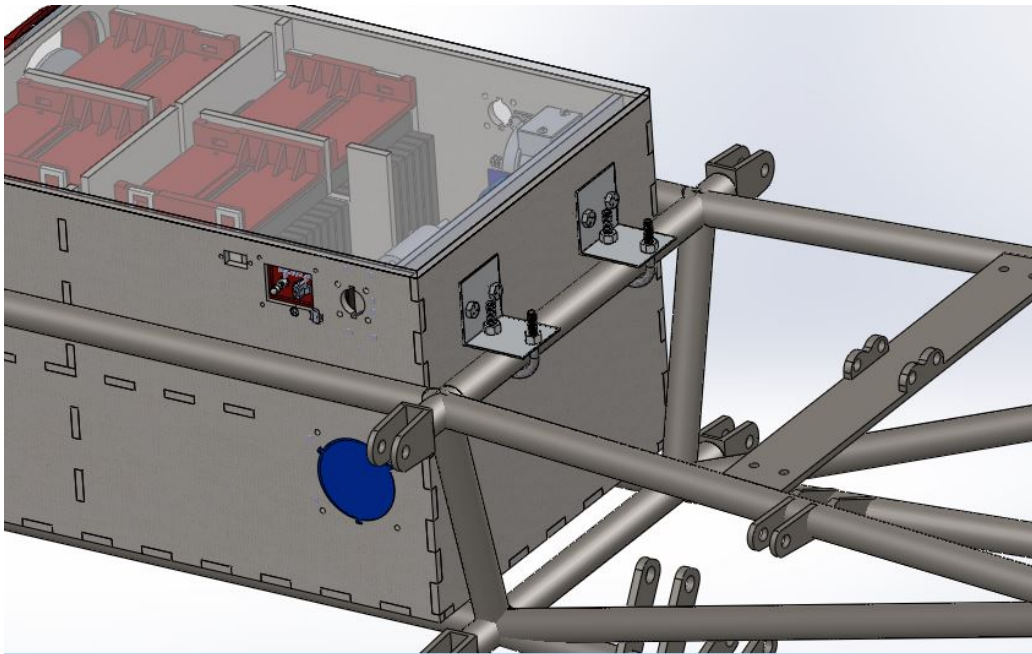


Figure 19. Attachment Points from Battery Box to Chassis

The bare weight of the enclosure and insulation is 0.9kg. Airflow is provided by two 80mm computer fans drawing and expelling air through the air intake on the left wheel well and exhaust the right wheel well. The fans draw, in total, 1.84 watts at 1200 rpm.



Figure 20. Fully assembled singular battery module

## Battery Ventilation

Several fans will be used to direct airflow over the batteries with a total flow rate exceeding 280 L / min. The intake will follow the path marked in green on the diagram below, while the exhaust will follow the path marked in blue.

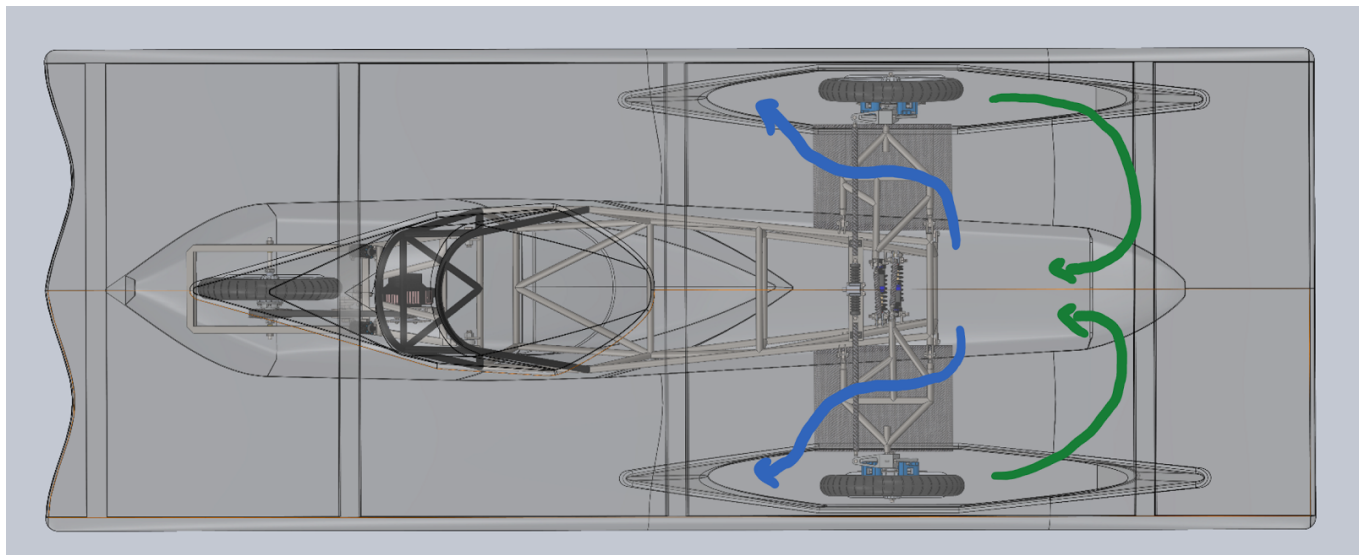


Figure 21. Battery Ventilation Diagram

## Loading Conditions

Since the battery enclosure fastens to the front of the rollcage, FEA analysis was performed to ensure that the enclosure will be sufficiently protected during a frontal impact case, which would be the most likely scenario to deform the battery enclosure. This is related to the first of the seven scenarios in the vehicle impact analysis and will be further discussed in that portion.

Another way that the battery box may fail is when the shear experienced by the walls of the battery box exceeds the maximum shear strength of the honeycomb at the area where the panels are bonded together. The honeycomb structure does very well at resisting compression, but as the chassis is absorbing most of the impact, we are not concerned about the normal compression strength.

## System Analysis

Material	Material Properties	Strength	Factor of Safety
Standard Cell Aramid Honeycomb	L-Shear Strength	1.207 MPa	7.4

There is a high factor of safety for the honeycomb structure to support the weight of the entire battery box enclosure with all the components under a 5G frontal impact.

## Seatbelts

### Overview

Our chosen seat belt system is a 5 points seat harness rated for racing purposes. Manufactured by Cipher Auto, it meets the SFI 16.1 standards, which meets racing standards and is typically used for drag racing or circle track racing.

The racing bucket will be constructed out of a folded metal sheet and a custom foam mold with extra padding for driver comfort. Critical attachment points of the lap belts will be located on a welded plate on the bottom of the rollcage and shoulder belts will be bolted onto a plate behind the driver that will also be welded.

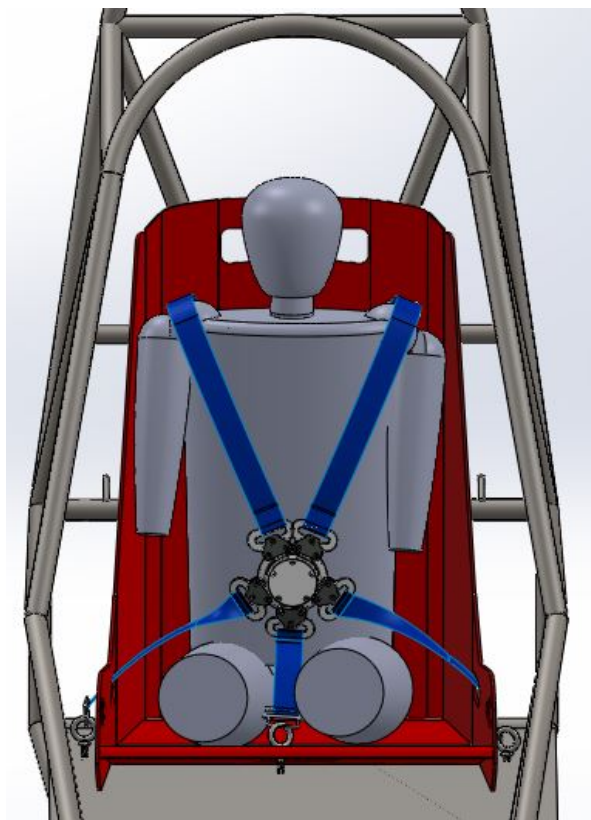


Figure 22- Front view, 5 point harness with approximate seat and human

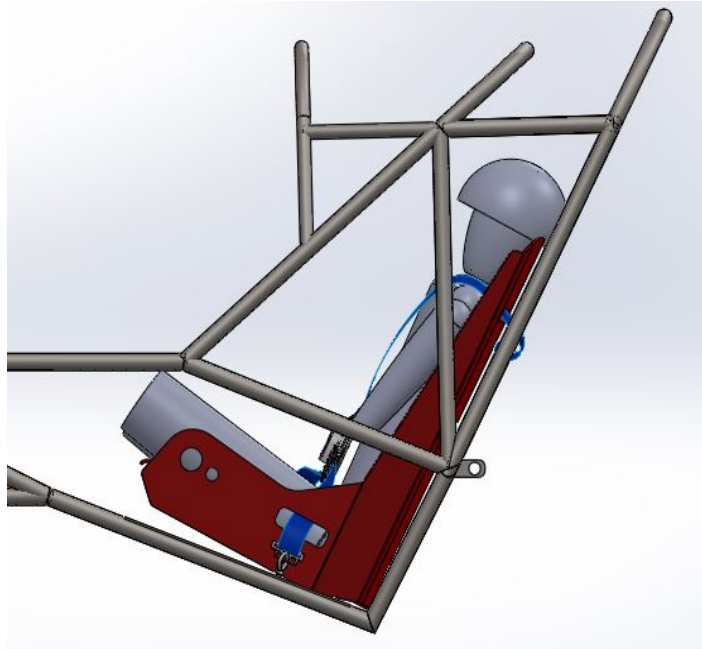


Figure 23- Side View, Lap belt and Shoulder belt attachment points

Part	Material/Details	Construction
Seatbelt Housing	Unknown	Manufactured by Retailer
Snap-Hook Belt Ends	SAE 1050 steel, Cadmium Plated	
Belts	Heavy Duty Nylon Webbing	

Part	Material/Details	Construction
Seat	1/16" Mild Steel Sheet	Waterjet and bent
	Foam-It! Expanding foam	Molded and bonded to seat
Mounting Points	1/4" 4130 Chromoly Steel Sheet	Waterjet and TIG-welded

## Loading Conditions

---

The primary load that the seat belts need to support is the driver's weight under different scenarios.

### a.1G Braking

Under braking, the driver leans towards the direction of motion of solar car. We assume that the two shoulder straps will bear the entirety of the driver's weight with the ballast.

Part	Max Breaking Load (kg)	Factor of Safety
Shoulder Belt	2858	63

### b.1G Cornering

Although lap belts and the shoulder straps will hold her in, the driver's position is predominantly constrained by the sides of the seat.

### c. 2G Bumping

During bumping, the load will mainly be vertically. We will calculate the loading by assuming that the 2 lap belts and 1 submarine belt share 100% of the force experienced by the driver under 2G bumping.

Part	Max Breaking Load (kg)	Factor of Safety
Lap Belt	2858	46
Submarine Belt	680	11

# Vehicle Impact Analysis

## Specifications

### Overview

The vehicle chassis is a spaceframe type, fabricated from welded AISI 4130 (chromoly) 1" round tubes of two wall thicknesses: 0.083" for rollhoops and main structural members (outer truss members), and 0.065" for cross members (inner truss members). Chromoly members were TIG welded with ER70s2 filler rod. For driver protection, the chassis has dual rollhoops located overtop of the driver's compartment, and a third hoop of 0.03" wall thickness was added to provide extra structural support to the driver during rollover.

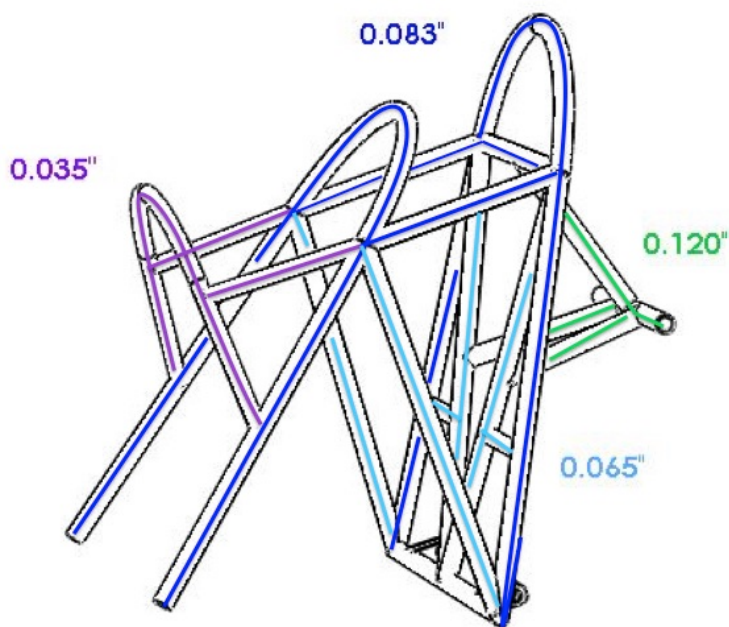
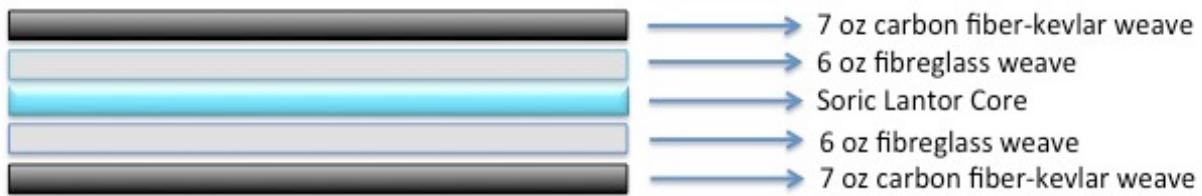


Figure 24. Isolated Rollcage & Rear Triangle with Different Wall Thicknesses

Surrounding the spaceframe is the aeroshell, which we consider non-structural. The aeroshell's main purpose is to provide a large surface area for the harvesting of solar power by monocrystalline solar panels on the topshell; and to enclose the rollcage in an aerodynamic structure. The wheel fairings and the a-arms are constructed in a similar fashion and also serve the purpose of improving vehicle aerodynamics.

The aeroshell is composed of five layers – from the inner to the outer layer. The combined thickness of the layup is approximately 3/16" (4.75mm). The binding material is an unwaxed polyester resin.

The rollcage will be attached to the aeroshell by bolts in aluminium plates, which are bonded to the bottom shell with sheets of carbon fiber and Kevlar weave.



**Figure 25. Layup schedule of Aeroshell**

Kevlar on the inner layer provides protection against aeroshell fragmentation in the event of a collision. Post-fracture carbon fibre breaks into shards while a carbon fibre/Kevlar weave fractures but the Kevlar fibres keep the fragments together. This was proved, on a small scale, by applying force to two samples each of 8x8" carbon fibre and carbon fibre/Kevlar. Force was applied in-plane to one set of samples sample, and through-plane to the other. Upon fracture of the resin, the carbon fibre shattered while the carbon/Kevlar crumpled. Given the Kevlar weave in the inner layer, in the case of collision and aerobody fragmentation it is unlikely that carbon fibre shards will impact the driver.

The aeroshell has three supporting ribs that go across the width of the bottom shell and the top shell. We used high density foam and bonded carbon fiber to the shell in the same layup schedule as the rest of the aeroshell, as described above.

For the crush zone, we will be using the IMPAXX™ 700 Energy Absorbing Foam, which is specifically developed for high efficiency energy absorption in automotive applications. It is typically used as a passive barrier for side impact collisions due to its compressive stress-strain curve resembling that of an ideal energy absorber.

## Drawings

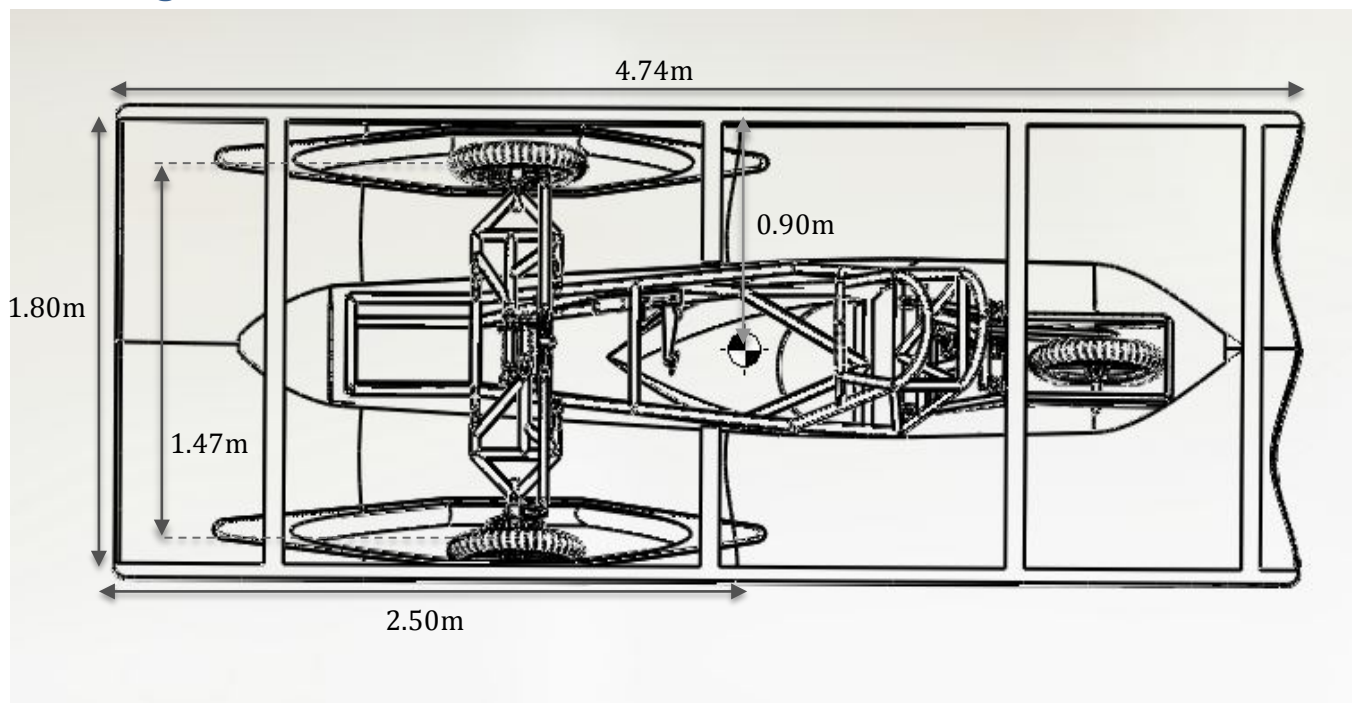


**Figure 26. Top view of Chassis and Aeroshell**

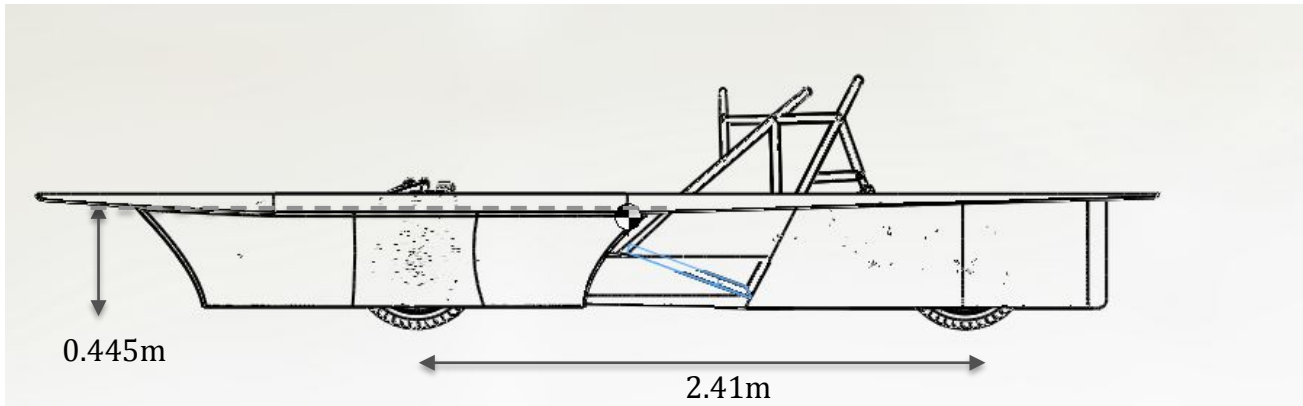


Figure 27. Side view of Aeroshell and Chassis

There are two main towing hardpoints, one of which is welded onto the main rollcage. It is a triangular structure with one upper brace and two horizontal braces. All tubes in the rollcage triangle are made from 1" OD and 0.120" wall thickness. The other towing hard point is located on the mid point of the first rib of the bottomshell.

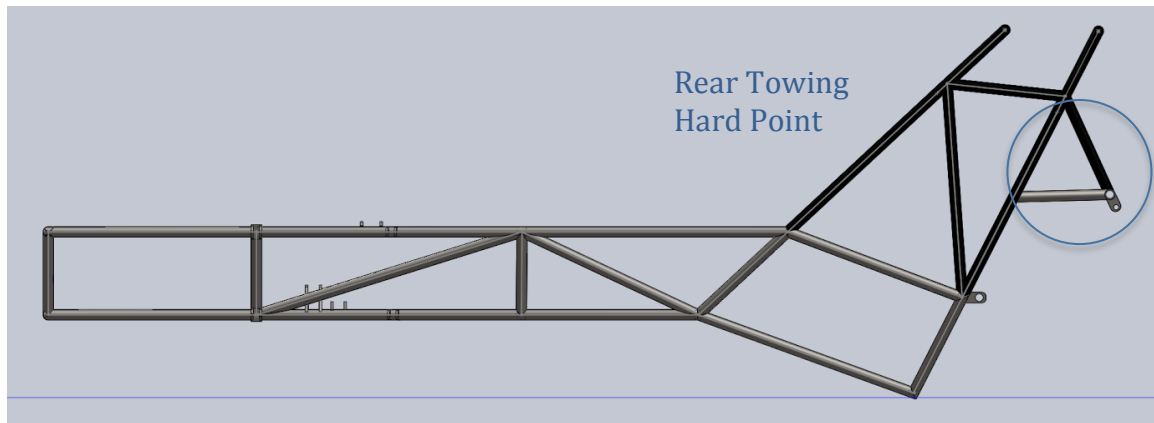


Figure 28. Side View of Rollcage (Main Structural Component)

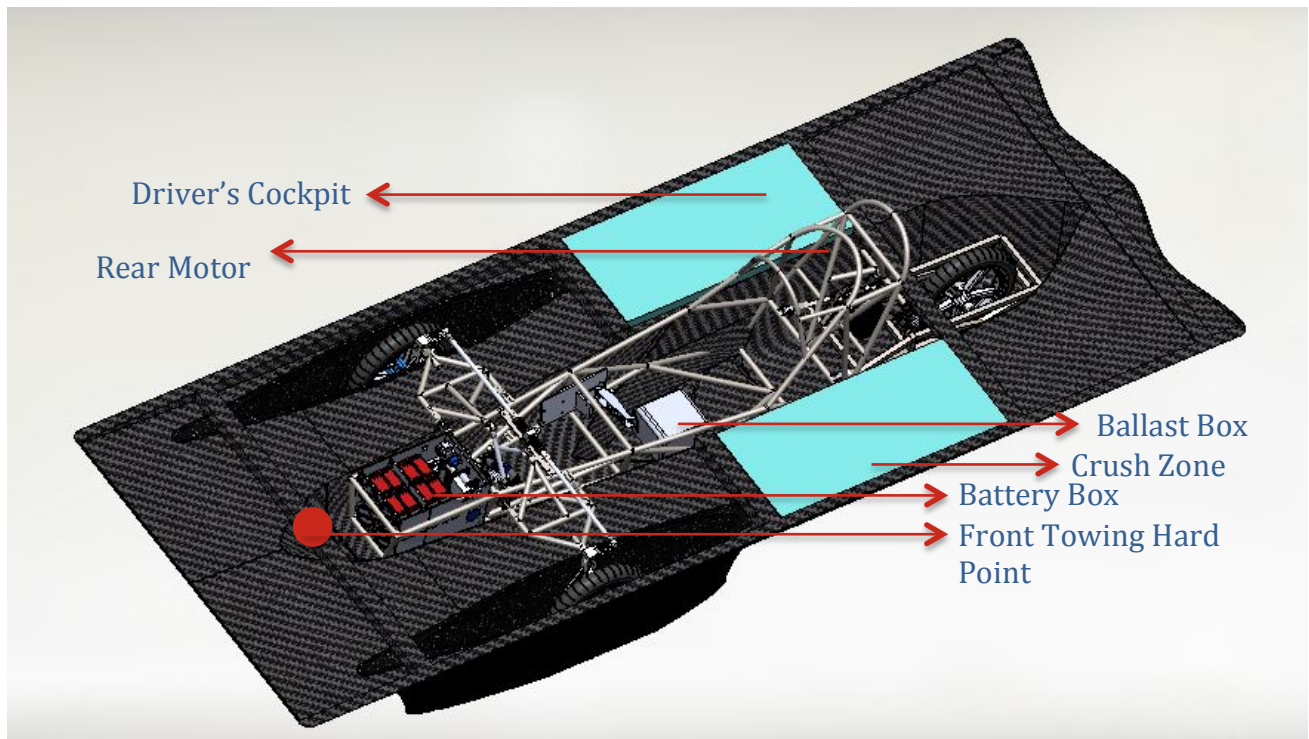


Figure 19. Position of Critical Components

## Centre of Gravity

Estimated centre of gravity with the driver and ballast in position.

X	From the front edge of the Aeroshell	158 cm
Y	From the side edge of the Aeroshell	87 cm
Z	From the ground (contact patch of tires)	44.5 cm

This is only an estimate of our centre of gravity, as the car is not fully assembled yet. In the near future, we will be finding a more accurate centre of gravity by means of empirical testing.

Once the car is fully assembled, with the driver in the cockpit, we will be placing one scale on each of the three wheels and record this initial reading. Then, we will raise the rear wheel 12 inches off the level surface and record the new readings on the three wheels. With this difference, we will be able to calculate the new centre of gravity<sup>[1]</sup>.

<sup>[1]</sup>W.F. Milliken & D.L. Milliken. [Race Car Vehicle Dynamics], Section 18.2. (1995).

## Analysis & Conclusions

Stress, displacement, and factor of safety simulations for eight impact scenarios (As shown in the figure below from the FSGP Regulations) were performed in ANSYS using the Static Structural solver and assuming 580lb vehicle weight. This is approximately equal to a 13000N force being applied over a short period. In the images that follow, orange arrows are applied forces, and red X's are rigid supports.

Due to the non-structural nature of the aeroshell, the rollcage will be taking the most load during impacts and will be the primary safety structure for the driver. As the aeroshell will crumple without shattering under direct impact, hence the ability of the rollcage to withstand impacts from different directions is the utmost importance to driver protection. The third rollcage hoop will not be included as it is not the main structural support for driver safety.

### Scenario 1: 5G Front Impact

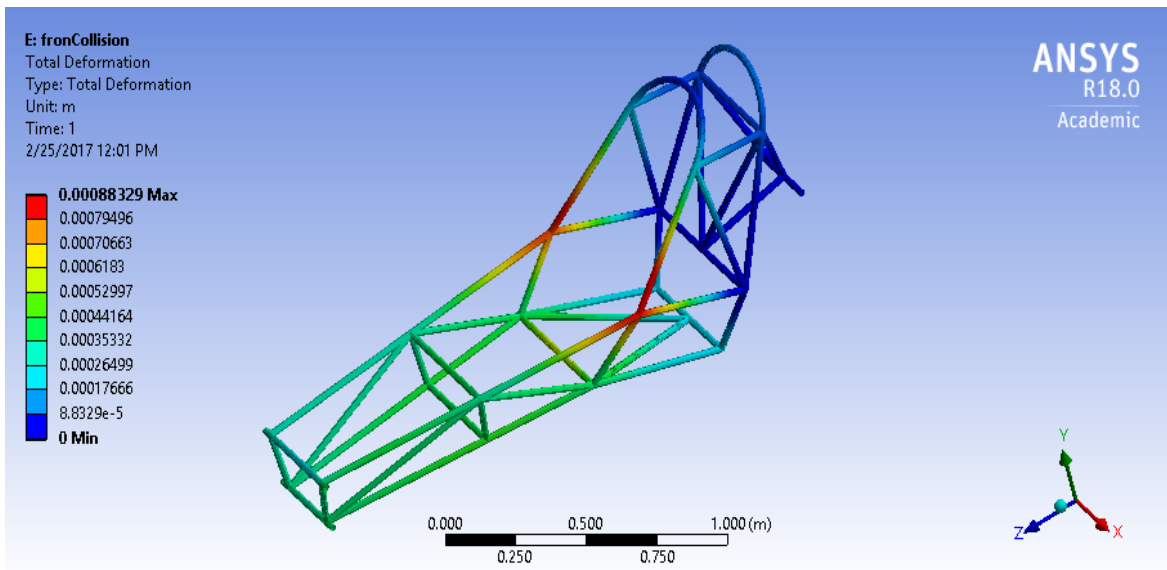


Figure 30. Deformation due to 5G Frontal Impact

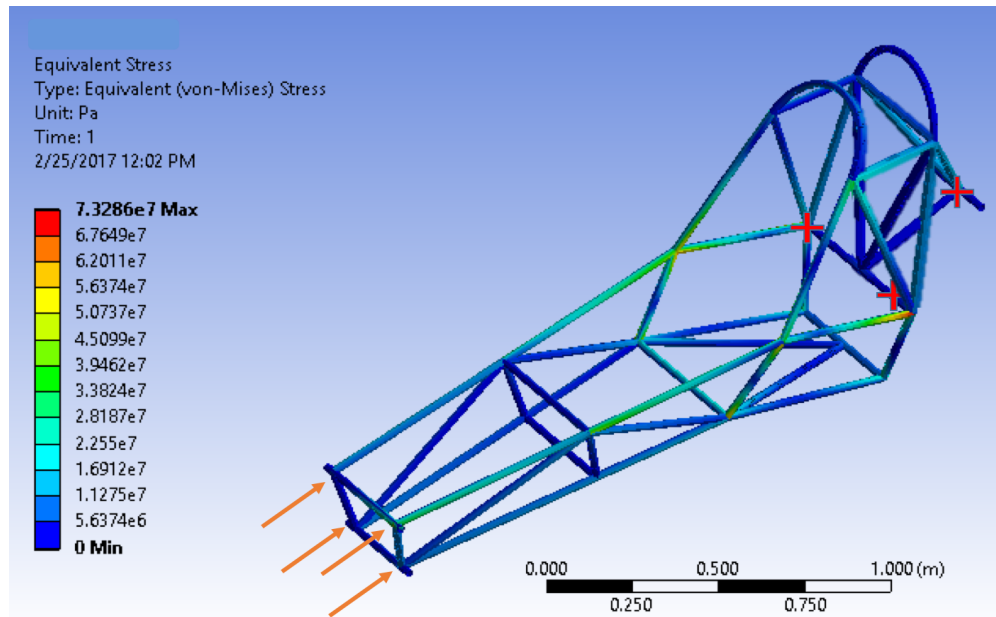


Figure 31. Von Mises Stress Distribution on Roll cage from 5G Frontal Impact

<b>Maximum Displacement</b>	<b>0.883mm</b>
<b>Maximum Von Mises Stress</b>	<b>73.3MPa (460MPa Yield)</b>
<b>Factor of Safety</b>	<b>6.3</b>

The front impact by a 10cm high bumper 35cm from the ground is absorbed by the two main truss sections of the chassis and has very little effect on the car. Both displacement and probability of failure are very low. The fixed supports are placed where the rear wheel and suspension assembly is mounted on the chassis via tabs because this is where the car would be stopped if it were longitudinally sandwiched by the collision and a wall or other

constraint. Also, maximum displacement is not at the front of the rollcage, and hence the battery box can be assumed to be adequately protected by the frame.

### Scenario 2: 5G Impact at a slight angle from the front

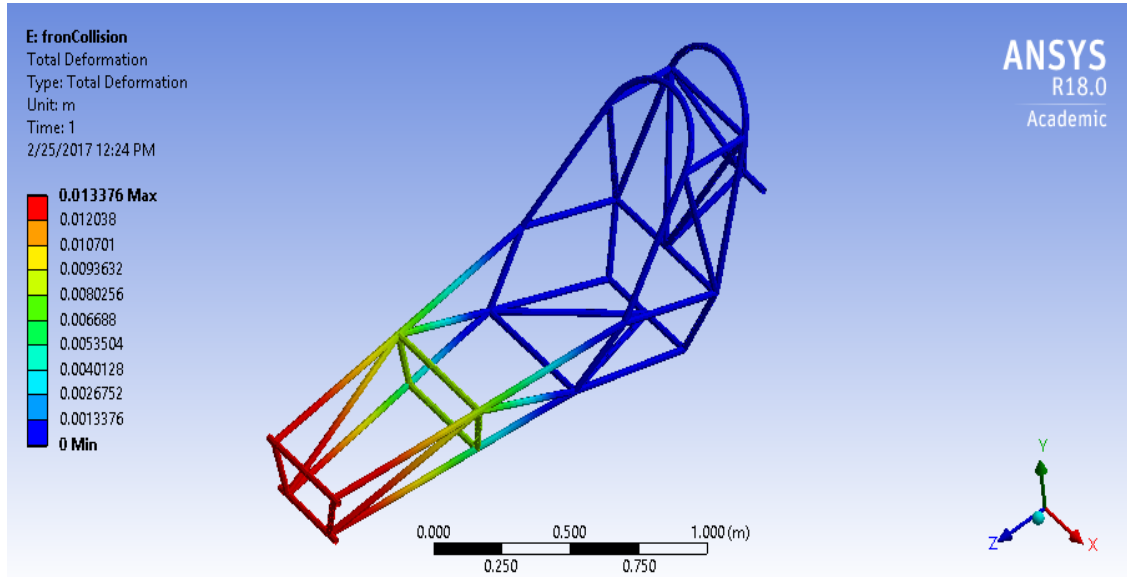


Figure 32. Deformation stress due to 5G Impact from the Side

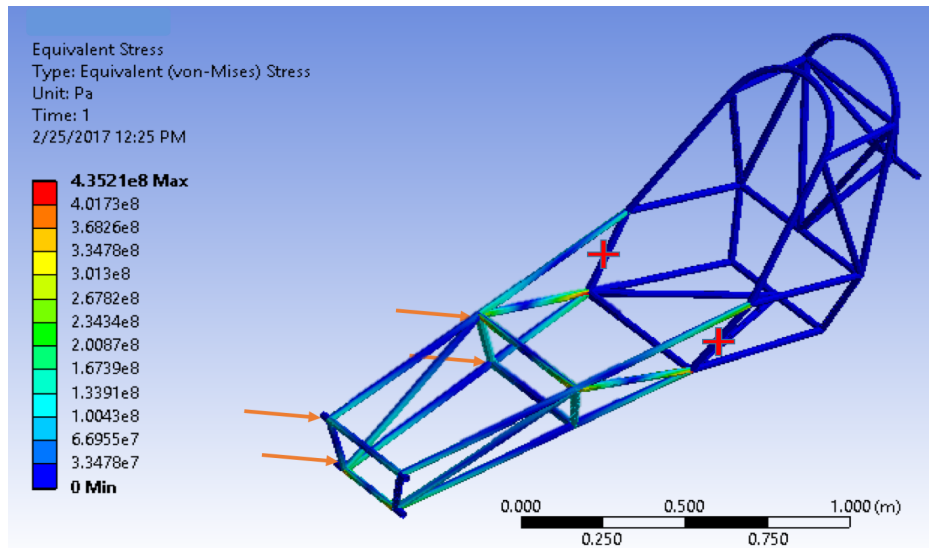


Figure 22. Von Mises Stress due to 5G Impact at slight angle from side

<b>Maximum Displacement</b>	1.33cm
<b>Maximum Von Mises Stress</b>	435MPa (460MPa Yield)
<b>Factor of Safety</b>	1.1
<b>Angle used</b>	45° from the front

This appears much more severe than it actually would be because in reality the car would simply be deflected by the collision and rotate away, thus drastically lowering the forces involved. However, in ANSYS, the car is fixed in space, causing the impact to seem severe.

This is an almost unimaginable worst case scenario. Furthermore, the aeroshell and wheels will greatly decrease the impact felt by the chassis. The frame surrounding the driver has very little stress or deformation, so the driver will still be safe.

### Scenario 3: 5G Side Impact

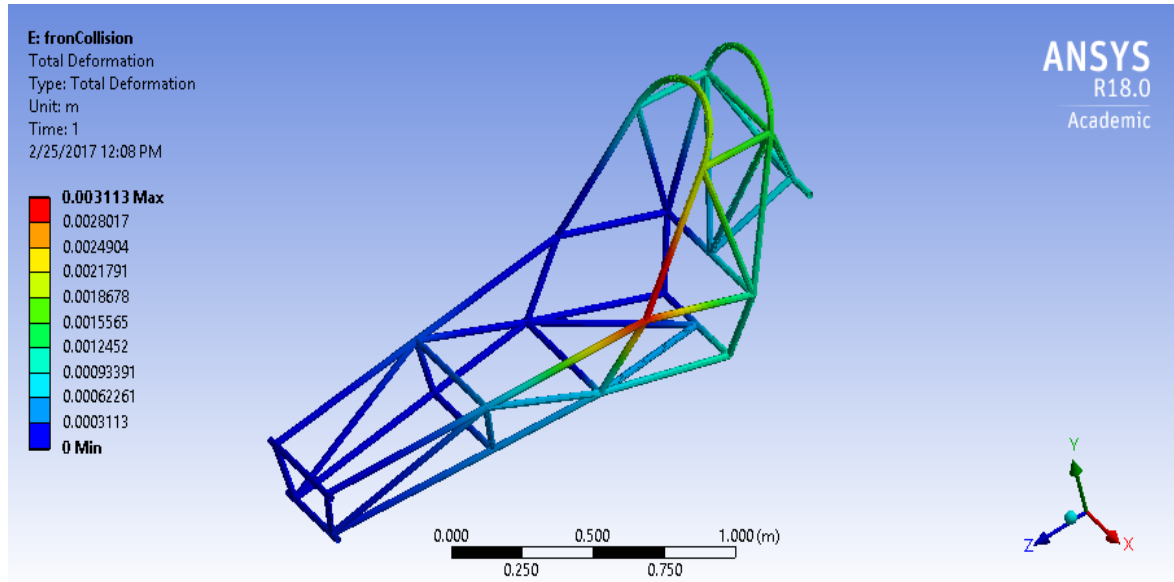


Figure 34. Total Deformation from 5G Side Impact

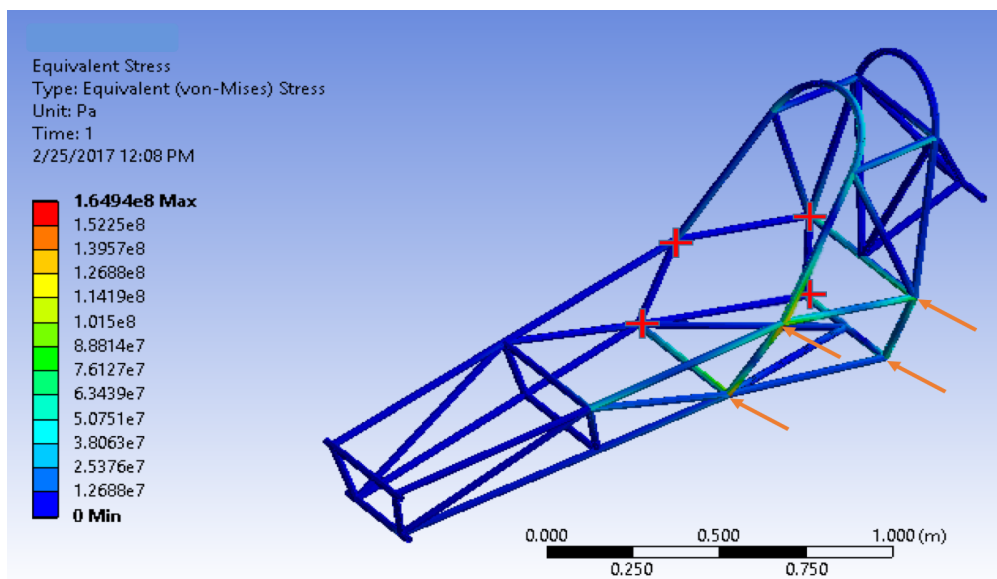


Figure 35. Von Mises Stress from 5G Side Impact

<b>Maximum Displacement</b>	<b>7.88mm</b>
<b>Maximum Von Mises Stress</b>	<b>283MPa</b>
<b>Factor of Safety</b>	<b>(460MPa Yield)</b>

This simulation is a very conservative estimate. We have assumed that there is a 5G impact from the side with the other side of the rollcage fixed. We have also not considered the ample crumple zone provided by both the aeroshell and the crush zone.

### Scenario 4: 5G Rear Impact

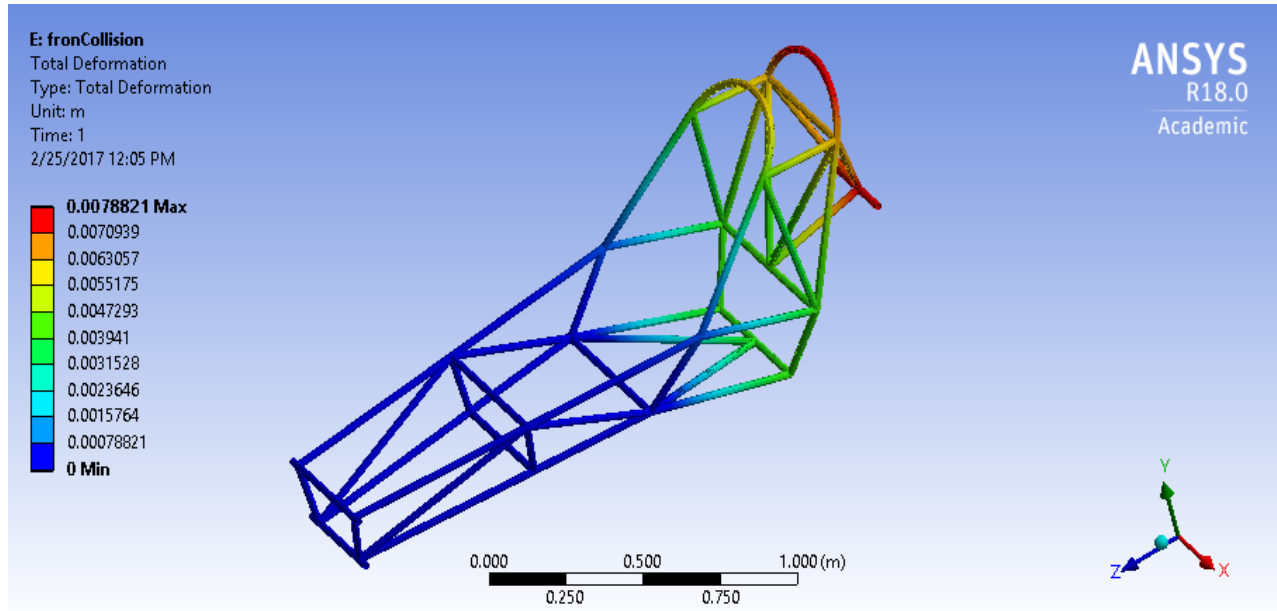


Figure 36. Deformation Stress under 5G Rear Impact on Rollcage

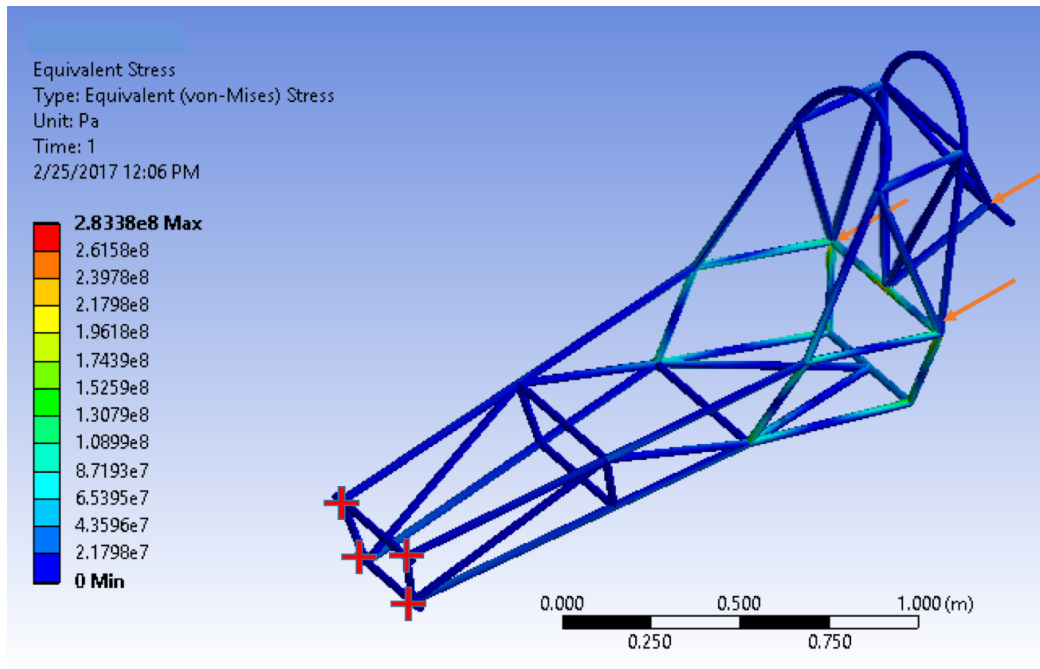


Figure 37. Von Mises Stress Distribution under 5G Rear Impact on Rollcage

<b>Maximum Displacement</b>	<b>5.73mm</b>
<b>Maximum Von Mises Stress</b>	416MPa (460MPa Yield)
<b>Factor of Safety</b>	1.1

Realistically simulating a rear-impact is difficult since any such collision would transmit forces through the drive-wheel, into the suspension and chassis. This transmission of the forces is modelled here by applying the forces on the points where the drive wheel and suspension attach to the chassis through tabs. The maximum displacement occurs is the most severe at the rear rollcage triangle, which is a structural member and will be able to provide structural support to the driver's back during the collision.

### Scenario 5: 5G Forward Rollover Impact

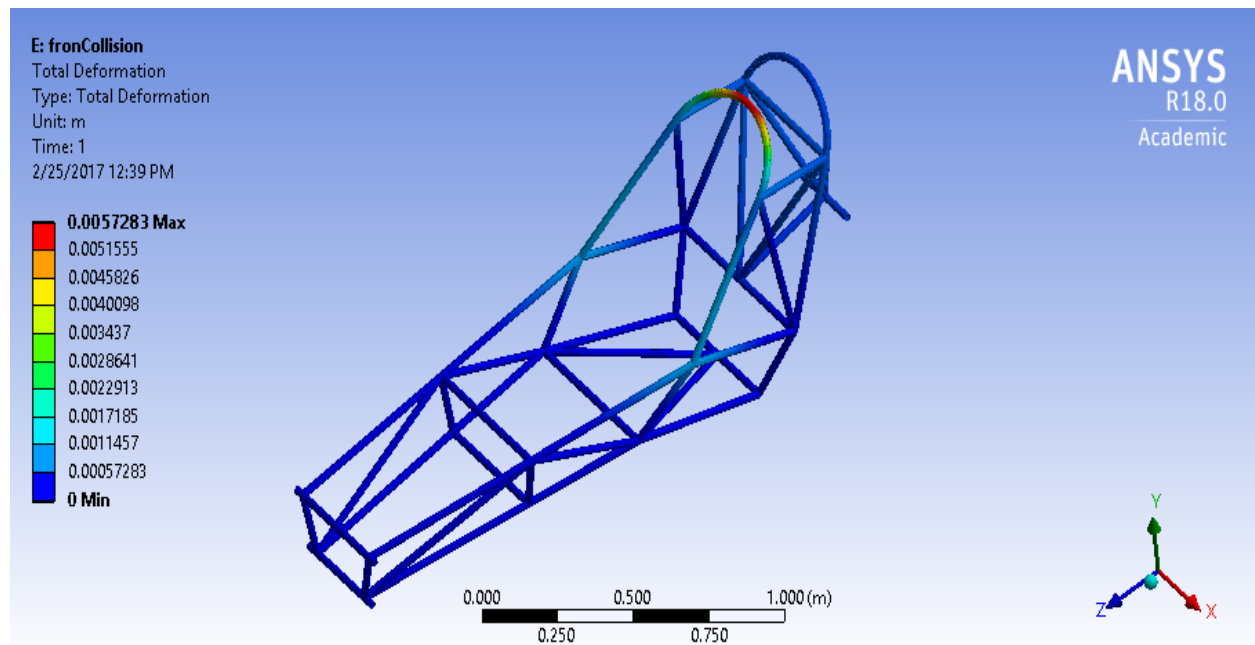


Figure 38. Deformation Stress due to 5G Rollover on Rollcage

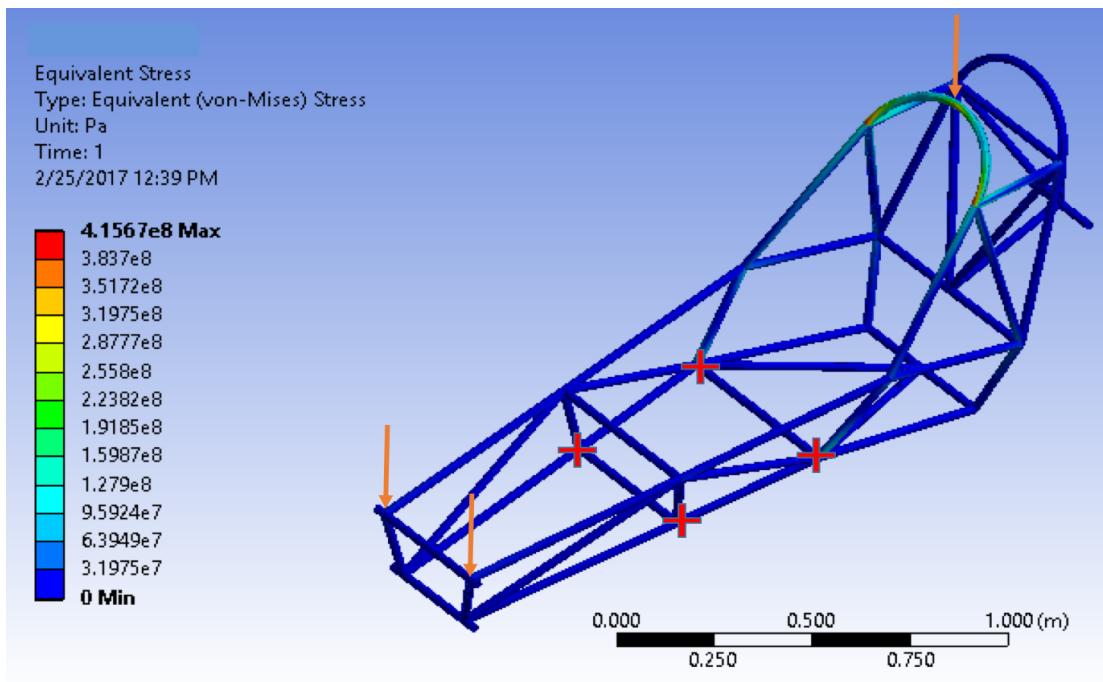


Figure 39. Von Mises Stress Distribution on Rollover

The results show a small displacement with substantial stress on the front rollhoop. Though the stress is still below the yield stress, the force would realistically be shared between the third hoop and the first largest hoop and the factor of safety will be larger than 1.1

### Scenario 6: 5G Side Rollover Impact (1<sup>st</sup> Stage)

The next three simulations represent the three stages in rollover. First, the car is flipped on its side, then almost upside down, then fully upside down.

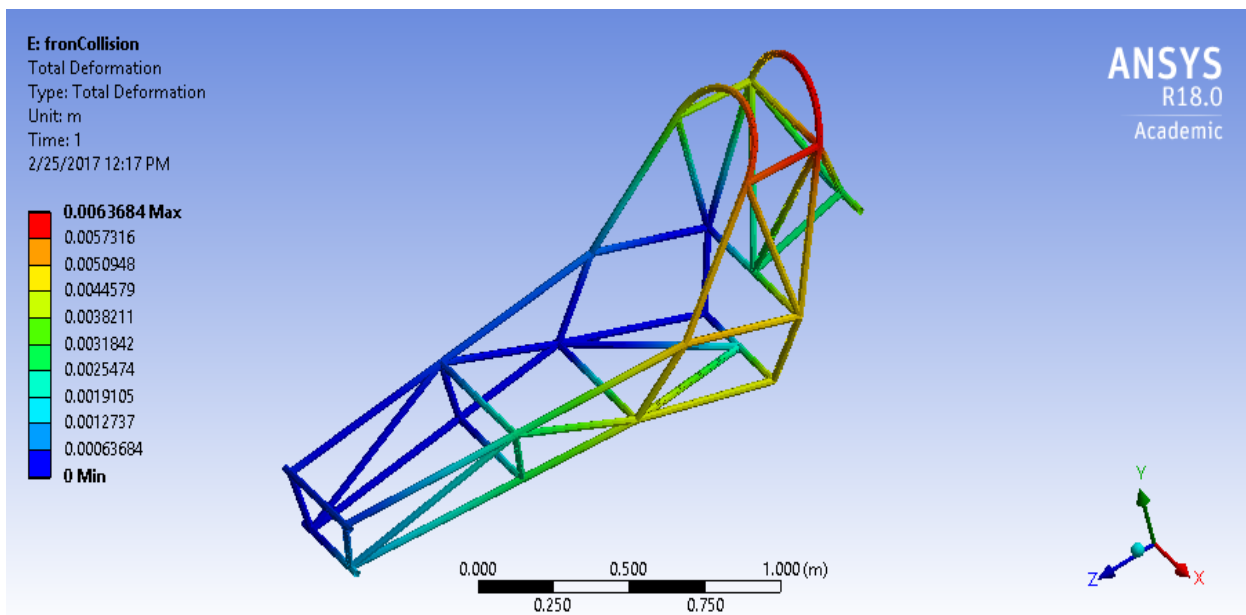
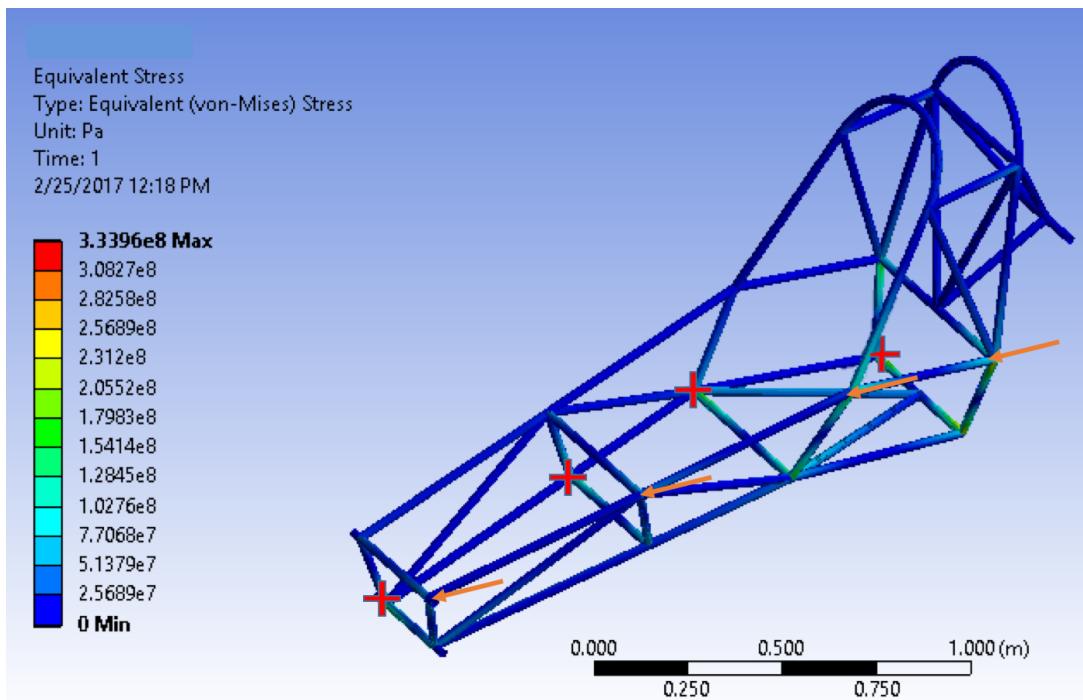


Figure 40. Deformation Stress due to Side Rollover on Rollcage



**Figure 41. Von Mises Stress Distribution due to Side Rollover on Rollcage**

<b>Maximum Displacement</b>	<b>6.37mm</b>
<b>Maximum Von Mises Stress</b>	334MPa (460MPa Yield)
<b>Factor of Safety</b>	1.4

This simulation will not be able to show the effects of a roll as it treats the forces in each stage as a direct impact. Thus, the stress is actually much lower and less direct than is shown in these simulations. The FOS in the first stage is high enough, and the displacement is also safe for the driver. A maximum displacement of 6mm leaves another 44mm of space between the chassis and the driver's helmet, which is still a safe distance.

## Scenario 7: 5G Side Rollover Impact (2<sup>nd</sup> Stage)

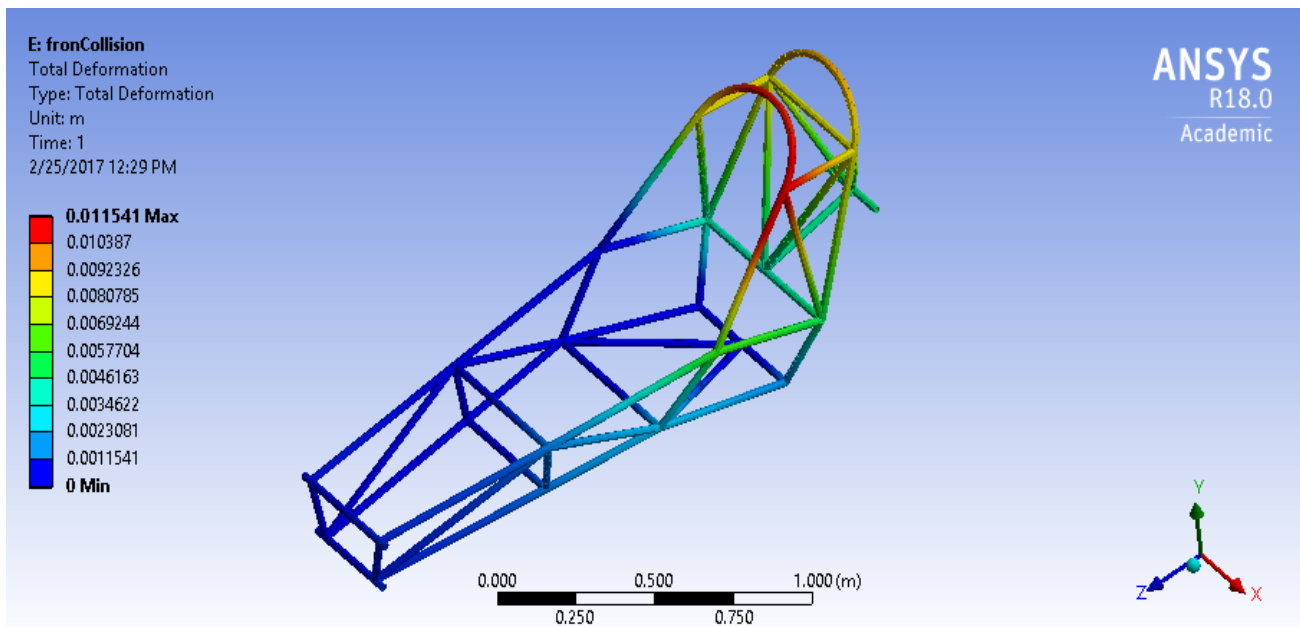


Figure 42. Deformation Stress due to Side rollover on the rollcage.

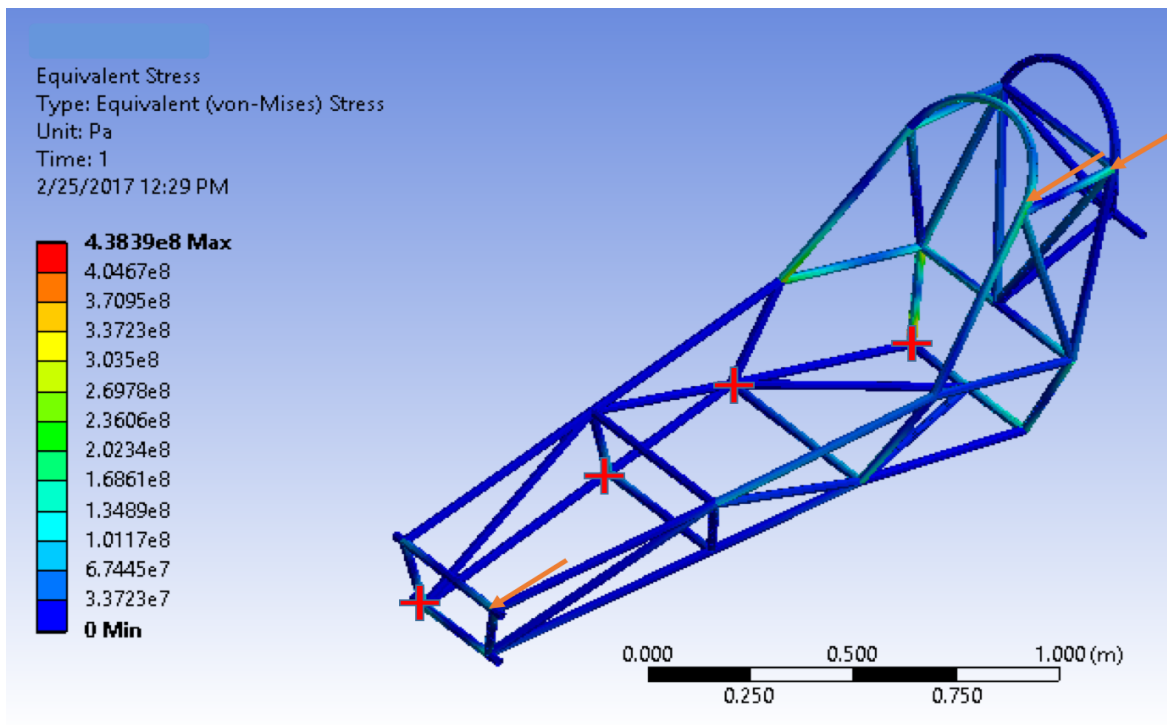


Figure 43. Von Mises Stress Distribution due to second stage of side rollover

<b>Maximum Displacement</b>	<b>1.15cm</b>
<b>Maximum Von Mises Stress</b>	<b>438MPa (460MPa Yield)</b>
<b>Factor of Safety</b>	<b>1.1</b>

As explained in stage one, these stress and displacement numbers are unrealistically high. Rather than having this large force directly onto the chassis as shown, the chassis would be rolling over, and the stress would evolve more gently over time. However, the results still show a fairly small displacement at the high stress and keeping in mind the unrealistic nature of the simulation, an FOS of 1.1 is not bad as it shows that the chassis will hold up in much worse circumstances than are realistically probable or even possible. Furthermore, the driver still has close to 4cm of clearance between his helmet and the chassis even in this extreme over approximation.

### Scenario 8: 5G Side Rollover Impact (3<sup>rd</sup> Stage)

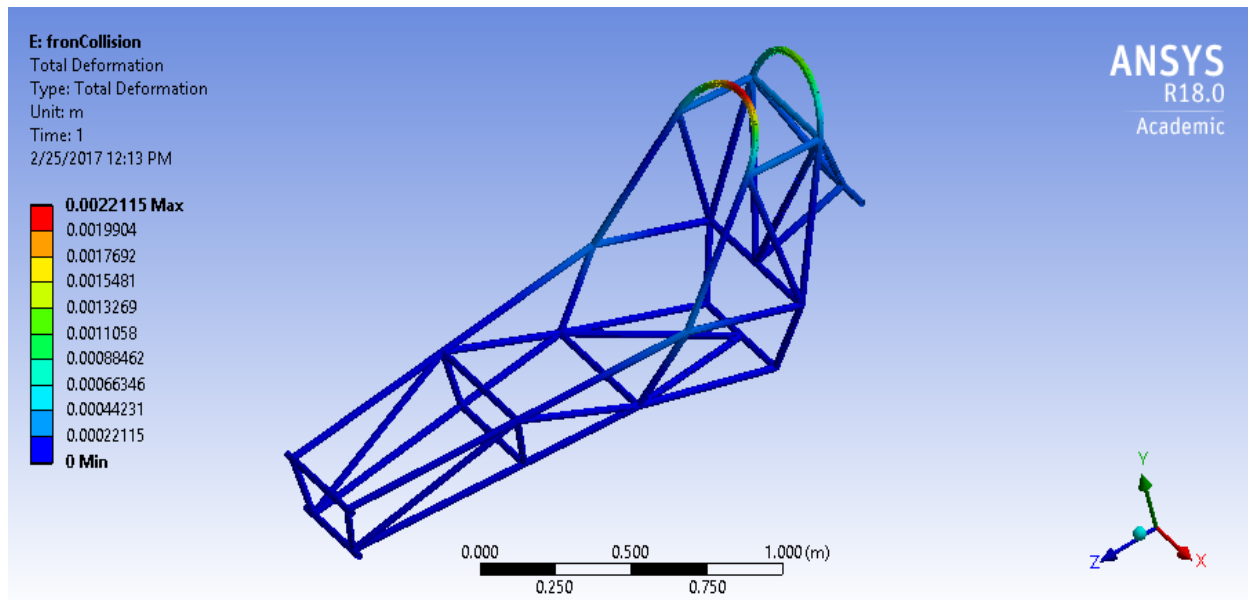


Figure 44. Deformation Stress due to side rollover impact on rollcage

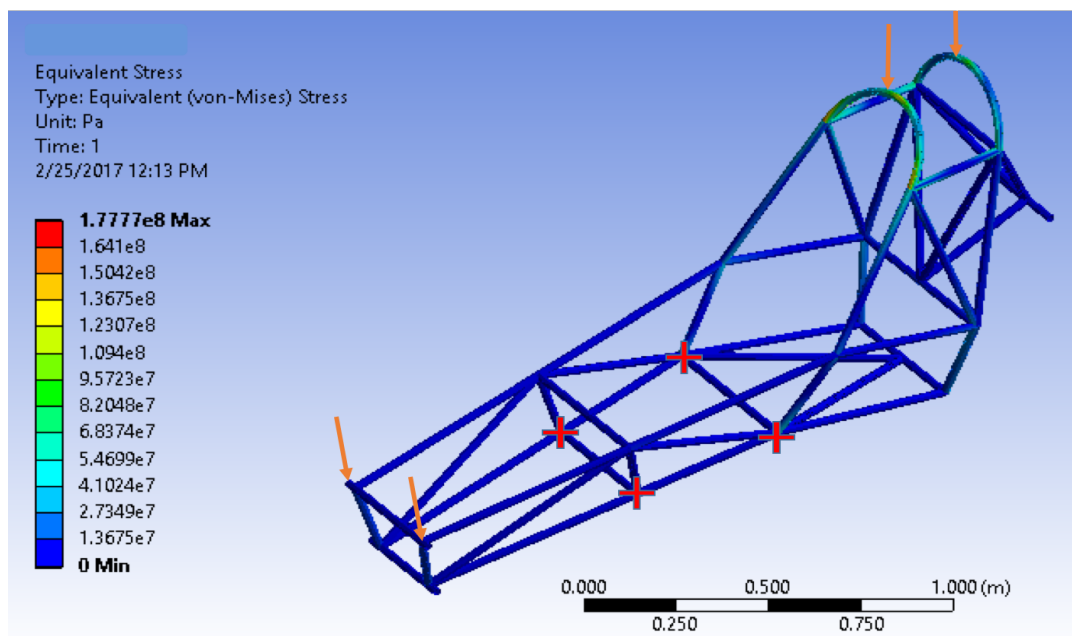


Figure 45. Von Mises Stress due to side rollover impact (stage three)

<b>Maximum Displacement</b>	<b>2.21mm</b>	
<b>Maximum Von Mises Stress</b>	178MPa	(460MPa Yield)
<b>Factor of Safety</b>	2.6	

A very small displacement in the tubing after impact protects the driver's head well. Considering the large overestimate in stress that these simulations represent, it is apparent that the driver will be completely safe in a rollover situation.

## Conclusion

In order to carry out these simulations, we were forced to make a number of assumptions, all outlined above. All of the assumptions, however, served to make the given impact scenarios more severe than they would be in reality. All the same, the chassis withstood every test, usually with ease, and in every simulation the driver safety was very high due to small displacements of the chassis around the driver. Therefore, we can safely conclude that the car will be able to withstand any impact it would reasonably be subjected to while keeping the driver safe. For more details on each simulation, see Appendix B.

# APPENDIX A

## MECHANICAL SYSTEMS ANALYSIS

### Front Suspension

Weight of Car with Driver and Ballast	778	lbs	353	kg
Track Width	1.47	m		
Wheel Base	2.41	m		
Center of Gravity	0.445	m		
Weight Distribution	60	:	40	
coefficient of friction	0.8		(0.7-0.9)	

a: F1 distance from wheel center	0.26411	m
b: F2 distance from wheel center	0.06411	m
d: distance from center to ground	0.265	m
wheel & arm distances	0.51	m
upright & arm distance	0.43	m

### Forces on Front Suspension

#### Braking

$$F_v = (\text{Weight on front wheel} + \text{Longitudinal weight transfer}) * 9.81 \text{ ms}^{-2}$$

$$F_{fr} = \text{Coefficient of friction} * F_v$$

$$\text{Moment about Hub} = \text{Wheel radius} * F_{fr}$$

$$F1 * a + F2 * b = \text{Moment about Hub}$$

Turning 1g		
F <sub>v</sub>	1353	N
F <sub>fr</sub>	1082	N
Moment About Hub from friction	292	Nm
F1	216	N
<b>F2</b>	<b>3669</b>	<b>N</b>

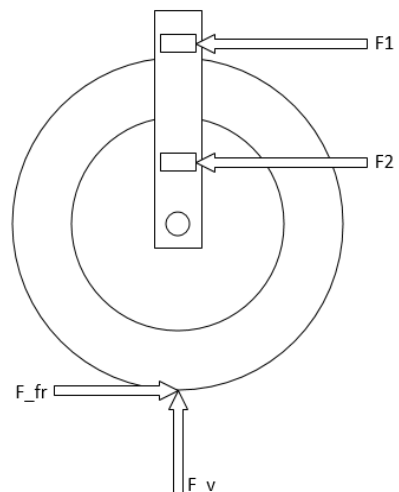


Figure 46. Braking Force Diagram

## Cornering

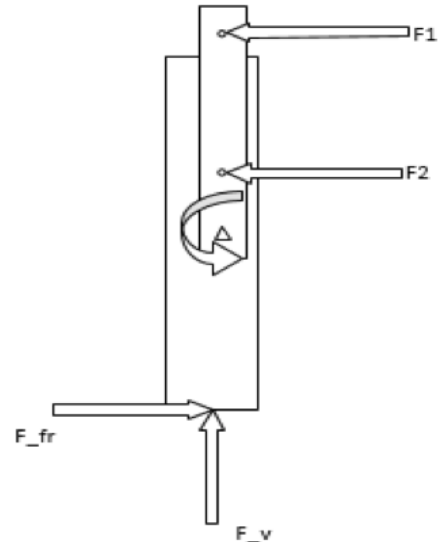
$$F_v = (\text{Weight on front wheel} + \text{Lateral weight transfer}) * 9.81 \text{ ms}^{-2}$$

$$F_{fr} = \text{Coefficient of friction} * F_v$$

$$\text{Moment about Hub} = \text{Wheel radius} * F_{fr}$$

$$F1 * a + F2 * b = \text{Moment about Hub}$$

Braking Condition @1g		
F_v	1198	N
F_fr	958	N
F1	191	N
F2	3249	N



## Bump

Figure 47. Cornering 1G Force Diagram

$$F_v = \text{Weight on front wheel} * 9.81 \text{ ms}^{-2} * 2$$

Bump 1g		
F_v	2077	N

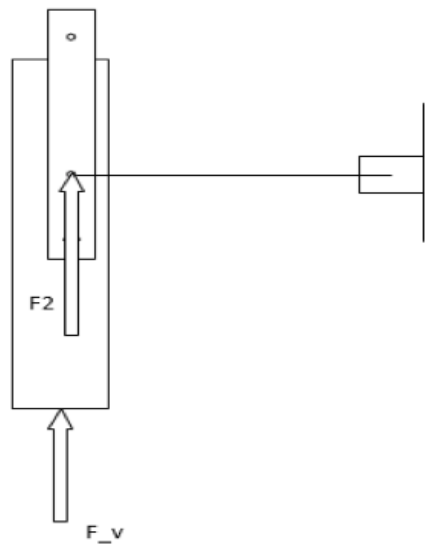


Figure 48. Bumping 2G Force Diagram

## Note:

Major assumptions: We are assuming that the front suspension springs are stiff and there is negligible rotation at the rod end bearings to simplify calculations. We are also assuming a stiff chassis.

In the relevant calculations below, we combine the loadings from the front suspension from all three scenarios, where applicable, for each rod end bearing and bolt calculation.

## Bearing Loads

### Steel Double-Sealed Ball Bearings

---

Static Radial Load Rating: 549 kg

Each wheel hub houses two wheel bearings each.

Position	Max Load	Factor of Safety
Front Wheel (Static)	549	10.6
Rear Wheel (Static)	549	7.6

### Rod End Ball Bearings

---

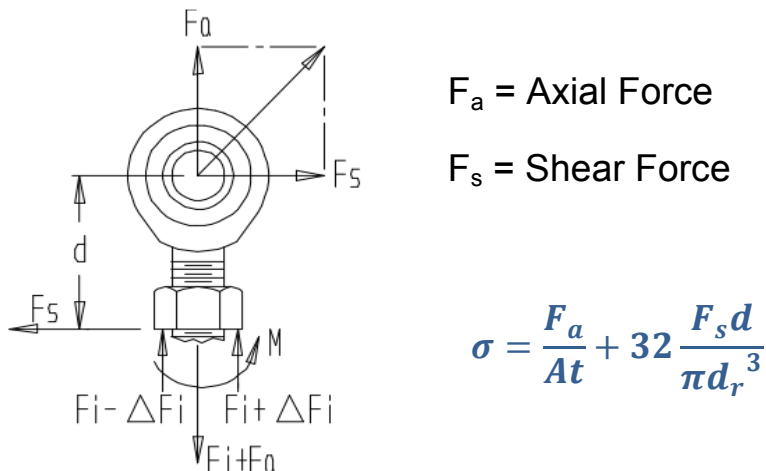


Figure 49. Forces on Rod End Bearing

$F_a$ : Axial Force;  $At$ : Tensile Area of Thread;  $F_s$ : Bending Force;  $d$ : Moment Arm

$d_r$ : Root Diameter of Thread

$$\eta = \frac{S_y}{\sigma}$$

$\eta$ : Factor of Safety;  $S_y$ : Yield Strength of Rod End;  $\sigma$ : Bending Stress

AM-5 ; $S_y = 131.5 \text{ ksi}$		
Position	Max Bending Stress	Factor of Safety
Top A-arms to Push Rods	684013549.8	4.2
Tie Rods to Upright		118.7

AM-7		
Position	Max Bending Stress	Factor of Safety
A-arms to Upright	650700633.6	13.58
A-arms to Chassis		13.58

AM-12		
Position	Max Bending Stress	Factor of Safety
Rear Swing Arm to Rollcage	438245400.7	31.53

## Bolt Calculations

Most of the bolts we are using are SAE Grade 5 bolts, which has a tensile strength of 120ksi.

$$\tau_y = K \cdot S_y$$

$\tau_y$  = Shear yield strength

$K$  = Relative Factor (changes with material type)

- for bolts this is approximately 60% of the minimum tensile strength

$S_y$  = Tensile yield strength

$$\tau_{eq} = F_{eq} / A_{tensile}$$

$\tau_{eq}$  = Equivalent shear stress

$F_{eq}$  = Equivalent force experienced by bolt

$A_{tensile}$  = Tensile stress area of bolt

$$SF = \tau_y / \tau_{eq}$$

$SF$  = Safety Factor

$\tau_y$  = Shear Yield Stress

$\tau_{eq}$  = Equivalent Shear Stress

✿ Bolt: 5/16"-24 UNF

Position		Factor of Safety
Front Wheel	Top A-arm to Push Rod	2.6
Brake	Brake Pedal Mount to Brake Pedal	13.1

✿ Bolt: 7/16"-20 UNF

Position		Factor of Safety
Front Wheel	Top A-arm and Upright	6.9
	Lower A-arm and Upright	5.7
	Top A-arm and Rollcage	8.2
	Lower A-arm and Rollcage	6.4

✿ Bolt: ½"-20 UNF

Position		Factor of Safety
Front Wheel	Top Bracket of Front Suspension Shocks	8.2
	Bottom Bracket of Front Suspension Shocks	8.2
Rear Wheel	Rear Suspension shocks	10.4

✿ Bolt: 3/4"-16 UNF

Position		Factor of Safety
Rear Wheel	Rear Swing Arm Frame to Rollcage	42.0

- ✿ Bolt: 3/8"-16 UNC

Position		Factor of Safety
Front Wheel	Brake Calliper Bolts	28.3

- ✿ Bolt: M8x1.125mm

Position		Factor of Safety
Motor	Motor to Motor Mount	81.3
Rear Wheel	Wheel Adaptor to Wheel Hub	33.6

## Steering

$$\text{Safety Factor} = \frac{S_s J}{T_{max} r} = 6.5$$

$S_s = 265.42 \text{ MPa}$  is the shear yield strength of chromoly  
 $J = 2.30 * 10^{-8} \text{ m}^4$   
 $r = 0.0135 \text{ m}$   
 $T_{max} = 70 \text{ Nm}$  is the moment applied by the driver

## Braking

$$\text{Wheel Static Pressure} = \frac{\text{Weight on Wheel} * g}{\text{Wheel Contact Patch}}$$

$$g = 9.81 \text{ ms}^{-2}$$

- ✿ 1G Braking Temperature

Variable	Description	Value
mcar	Mass of car	335 kg
mpad	Mass of brake pad	0.1 kg ( x8 pads )

mdisc	Mass of brake rotor	1.2 kg ( x2 pads )
Cpad	Specific heat of brake pad	935 J/kgK
Cdisc	Specific heat of brake rotor	449 J/kgK
v	Chosen speed of car	22m/s
T	Change in temperature	To find

$$E = Q$$

$$\frac{1}{2} m_{car} * v^2 = 8 * m_{pad} * C_{pad} * \Delta T$$

$$108C = \Delta T$$

The same calculation can be done with just the brake rotors which melting is around 1370°C.

$$E = Q$$

$$\frac{1}{2} m_{car} * v^2 = 2 * m_{disc} * C_{disc} * \Delta T$$

$$75^{\circ}C = \Delta T$$

## ⌚ 1G Braking Force

Variable	Description	Value
m	Mass of car	353 kg
r <sub>pedal</sub>	Brake pedal mechanical advantage	2.5
A <sub>pedal</sub>	Area of master cylinder piston	0.0001974705728 m <sup>2</sup>
A <sub>pad</sub>	Area of one brake pad	0.00155m <sup>2</sup>
C <sub>pad</sub>	Specific heat of brake pad	935 J/kgK
C <sub>disc</sub>	Specific heat of brake rotor	449 J/kgK
d <sub>rotor</sub>	Radius of the entire wheel	0.27"
d <sub>eff radius</sub>	Effective radius of the middle of the caliper piston to the center of the wheel	0.24"
f <sub>friction</sub>	Coefficient of friction between road & tire	0.8 (dry)

F	Force exerted by the driver	To be found
---	-----------------------------	-------------

$$\text{Pressure in Brake Lines} = \text{Pressure at Brake Pads} = \frac{F * r_{pedal}}{A_{pedal}}$$

*Force exerted by Brake Pads on one wheel*

$$= \text{Pressure in Brake Lines} * A_{pad} * 2 * c_{pad}$$

$$\text{Total Braking Force} = F_{\text{on one wheel}} * \frac{d_{rotor}}{d_{\text{eff radius}}} * 2 * c_{road}$$

By equating the total braking force to be 3345N, we worked backwards to find the force needed to be applied by the driver's foot- which is 405N.

## Battery Box

Below are some specifications from the manufacturer. We are mainly using the L shear strength to find the shear stress experienced by the panel.

Specification	Value
Compression	276 psi
L Shear Strength	175 psi
W Shear Strength	88 psi

The panel is experiencing single shear in the plane normal to the honeycomb panel.

$$\tau = \frac{F}{A_{shear}}$$

$$\text{Factor of Safety} = \frac{L_{shear}}{\tau}$$

## Wheels and Tires

Specification	Detail	Value
Centre of Gravity (X)	From the front of the Aeroshell	1.58m

Centre of Gravity (Y)	From the side of the Aeroshell	0.87m
Centre of Gravity (Z)	From the contact patch of the tire	0.45m
Track width	Between contact patches of two front tires	1.47m
Wheelbase	Between the front axles and the rear axle	2.41m
Weight of Car	With Driver and Ballast	353kg

### ✿ 1G Braking

$$\Delta W_x l = h W A_x$$

$$\therefore \Delta W_x = \frac{h}{l} W A_x$$

$\Delta W_x$  = Increase in rear axle downward load

$W$  = Weight of car

$h = z$  (height of center of gravity)

$l$  = Wheelbase

$A_x$  = Braking Acceleration

### ✿ 1G Cornering – Lateral Load Transfer

$$W_L = \frac{W}{2} + \frac{W A_y h}{t}$$

$$\Delta W = W_L - \frac{W}{2}$$

$W_L$  = Weight Load on outside tire of turn = 104.2 kg

$A_y$  = Cornering acceleration

$h = z$  (height of center of gravity)

$t$  = Track width

$\Delta W$  = Change in weight load

<b>Braking Acceleration</b>	<b>9.81</b>	<b>ms<sup>-2</sup></b>
Longitudinal Weight Transfer	65.9	kg
<b>Centripetal Acceleration (Cornering)</b>	<b>9.81</b>	<b>ms<sup>-2</sup></b>
Lateral Load Transfer (1g)	45.6	kg

# APPENDIX B

## Vehicle Impact Analysis Supporting Documentation

### General Settings

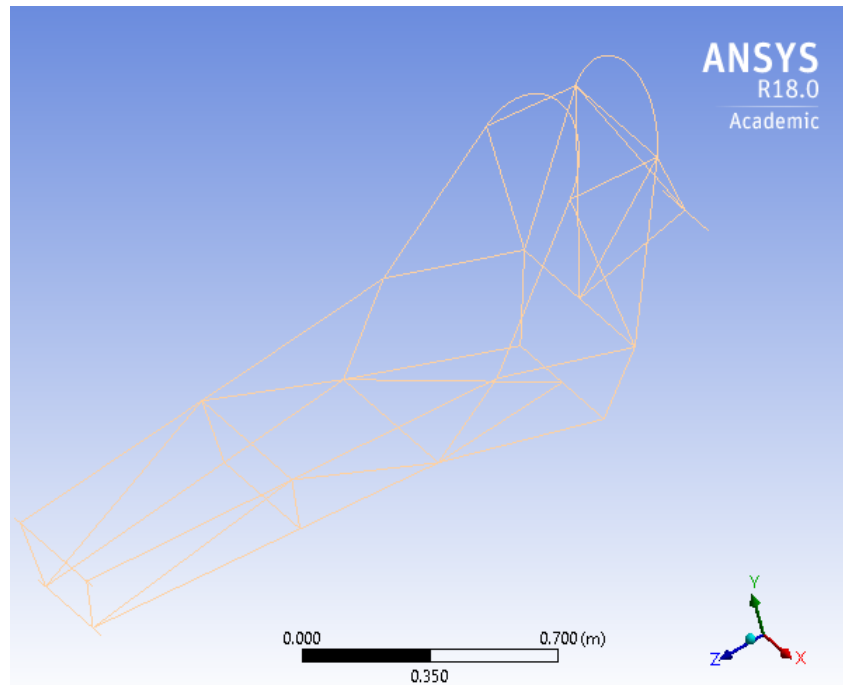


Figure 50. Imported line model in Ansys

### Mesh

Transition	Fast
Span Angle Center	Coarse
Curvature Normal Angle	Default (30.0 °)
Min Size	Default (8.9812e-003 m)
Max Face Size	Default (4.4906e-002 m)
Growth Rate	Default
Automatic Mesh Based Defeaturing	On
Defeature Size	Default (4.4906e-003 m)
Minimum Edge Length	6.2031e-006 m
Quality	
Check Mesh Quality	Yes, Errors
Error Limits	Standard Mechanical
Target Quality	Default (0.050000)
Smoothing	Medium
Mesh Metric	None
Inflation	

Use Automatic Inflation	None
Inflation Option	Smooth Transition
Transition Ratio	0.272
Maximum Layers	5
Growth Rate	1.2
Inflation Algorithm	Pre
View Advanced Options	No
Pinch Tolerance	Default (8.0831e-003 m)
Generate Pinch on Refresh	No
Sheet Loop Removal	No
<b>Statistics</b>	
Nodes	4562
Elements	2294

Object Name	<i>Edge Sizing</i>
State	Fully Defined
<b>Scope</b>	
Scoping Method	Geometry Selection
Geometry	57 Edges
<b>Definition</b>	
Suppressed	No
Type	Element Size
Element Size	1.e-002 m
<b>Advanced</b>	
Size Function	Uniform
Behavior	Soft
Growth Rate	Default (1.850 )
Bias Type	No Bias

## Front Impact Scenario

<b>Definition</b>		
Type	Total Deformation	Equivalent (von-Mises) Stress
By		Time
Display Time		Last
Calculate Time History		Yes
<b>Results</b>		
Minimum	0.Pa	0.Pa
Maximum	8.8329e-004 m	7.3286e+007 Pa

## Front Angled Impact Scenario

Definition		
Type	Total Deformation	Equivalent (von-Mises) Stress
By		Time
Display Time		Last
Calculate Time History		Yes
Results		
Minimum	0.Pa	0.Pa
Maximum	1.3376e-002 m	4.3521e+008 Pa

## Side Impact Scenario

Definition		
Type	Total Deformation	Equivalent (von-Mises) Stress
By		Time
Display Time		Last
Calculate Time History		Yes
Results		
Minimum	0.Pa	0.Pa
Maximum	2.6457e-003 m	1.3951e+008 Pa

## Rear Impact Scenario

Definition		
Type	Total Deformation	Equivalent (von-Mises) Stress
By		Time
Display Time		Last
Calculate Time History		Yes
Results		
Minimum	0.Pa	0.Pa
Maximum	7.8821e-003 m	2.8338e+008 Pa

## Front Rollover Scenario

Definition		
Type	Total Deformation	Equivalent (von-Mises) Stress
By		Time
Display Time		Last
Calculate Time History		Yes
Results		
Minimum	0. m	0. Pa
Maximum	5.7283e-003 m	4.1567e+008 Pa

## Side Rollover Stage 1

Definition		
Type	Total Deformation	Equivalent (von-Mises) Stress
By		Time
Display Time		Last
Calculate Time History		Yes
Results		
Minimum	0.Pa	0.Pa
Maximum	8.8063e-003 m	3.8612e+008 Pa

## Side Rollover Stage 2

Definition		
Type	Total Deformation	Equivalent (von-Mises) Stress
By		Time
Display Time		Last
Calculate Time History		Yes
Results		
Minimum	0.Pa	0.Pa
Maximum	1.1541e-002 m	4.3839e+008 Pa

## Side Rollover Stage 3

Definition		
Type	Total Deformation	Equivalent (von-Mises) Stress
By		Time
Display Time		Last
Calculate Time History		Yes
Results		
Minimum	0.Pa	0.Pa
Maximum	2.2115e-002 m	1.7777e+008 Pa